and *in vivo* (3,24). As shown in Fig. 4, the AAVtk/GCV system effectively killed the cancer cells depending on the concentration of GCV. Furthermore, when the cancer cells were treated with topoisomerase inhibitors prior to transduction, they were killed more efficiently in a concentration-dependent manner (Figs. 5 and 6).

The combination therapy using other vectors and chemotherapy have been reported (15,33), but the augmentation of the second-strand synthesis by chemotherapeutic agent is unique to AAV vectors. Favorably, apoptosis induced by topoisomerase treatment enhance the bystander effects, which may allow nearby untransduced cells to take up the apoptotic vesicles containing phosphorylated toxic GCV metabolites. Thus, the combination therapy of AAV-mediated suicide gene therapy with chemotherapeutic agents or other genotoxic stress such as radiotherapy seems to be valuable for the treatment of cancers.

Recently, the HSVtk mutants with improved GCV mediated killing and bystander effect have been developed (34,35). Since GCV has side effects such as pancytopenia and acute renal failure, the concentration of GCV should be kept as low as possible. Our model would be another alternative to improve AAV-mediated suicide gene therapy of cancer. Although several studies were reported on combining chemotherapy and viral vector-mediated gene therapy (15,33), our therapeutic model made it with acceptable concentrations of topoisomerase inhibitors. AAV-mediated suicide gene therapy and chemotherapy may provide a more effective and safer alternative for the treatment of head and neck cancer.

Acknowledgements

We thank Avigen Inc., for providing the plasmids, pAAVLacZ, pH19 and plAd5. We also thank the Cell Resource Center for Biomedical Research, Tohoku University for providing the HEp-2 cells. This work was supported in part by grants from the Ministry of Health, Labor and Welfare of Japan, Grants-in-Aid for Science Research from the Ministry of Education, Culture, Sports, Science and Technology of Japan, and Special Co-ordination Funds for promoting Science and Technology of the Science and Technology Agency of the Japanese Government.

References

1. Hamstra DA, Rice DJ, Fahmy S, Ross BD and Rehemtulla A: Enzyme/prodrug therapy for head and neck cancer using a catalytically superior cytosine deaminase. Hum Gene Ther 10: 1993-2003, 1999.
2. Clayman GL, El-Naggar AK, Roth JA, *et al*: *In vivo* molecular therapy with p53 adenovirus for microscopic residual head and neck squamous carcinoma. Cancer Res 55: 1-6, 1995.
3. Kanazawa T, Urabe M, Mizukami H, *et al*: Gamma-rays enhance rAAV-mediated transgene expression and cytocidal effect of AAV-HSVtk/ganciclovir on cancer cells. Cancer Gene Ther 8: 99-106, 2001.
4. Berns KI and Rose JA: Evidence for a single-stranded adenovirus-associated virus genome: isolation and separation of complementary single strands. J Virol 5: 693-699, 1970.
5. Blacklow NR, Hoggan MD, Sereno MS, *et al*: A seroepidemiologic study of adenovirus-associated virus infection in infants and children. Am J Epidemiol 94: 359-366, 1971.
6. Bueler H: Adeno-associated viral vectors for gene transfer and gene therapy. Biol Chem 380: 613-622, 1999.
7. Wagner JA, Reynolds T, Moran ML, *et al*: Efficient and persistent gene transfer of AAV-CFTR in maxillary sinus. Lancet 351: 1702-1703, 1998.
8. Muramatsu S, Fujimoto K, Ikeguchi K, *et al*: Behavioral recovery in a primate model of Parkinson's disease by triple transduction of striatal cells with adeno-associated viral vectors expressing dopamine-synthesizing enzymes. Hum Gene Ther 13: 345-354, 2002.
9. Kay MA, Manno CS, Ragni MV, *et al*: Evidence for gene transfer and expression of factor IX in haemophilia B patients treated with an AAV vector. Nat Genet 24: 257-261, 2000.
10. Ferrari FK, Samulski T, Shenk T and Samulski RJ: Second-strand synthesis is a rate-limiting step for efficient transduction by recombinant adeno-associated virus vectors. J Virol 70: 3227-3234, 1996.
11. Fisher KJ, Gao GP, Weitzman MD, De Matteo R, Burda JF and Wilson JM: Transduction with recombinant adeno-associated virus for gene therapy is limited by leading-strand synthesis. J Virol 70: 520-532, 1996.
12. Alexander IE, Russell DW and Miller AD: DNA-damaging agents greatly increase the transduction of non-dividing cells by adeno-associated virus vectors. J Virol 68: 8282-8287, 1994.
13. Russell DW, Alexander IE and Miller AD: DNA synthesis and topoisomerase inhibitors increase transduction by adeno-associated virus vectors. Proc Natl Acad Sci USA 92: 5719-5723, 1995.
14. Alexander IE, Russell DW, Spence AM and Miller AD: Effects of gamma irradiation on the transduction of dividing and non-dividing cells in brain and muscle of rats by adeno-associated virus vectors. Hum Gene Ther 7: 841-850, 1996.
15. Peng D, Qian C, Sun Y, Barajas MA and Prieto J: Transduction of hepatocellular carcinoma (HCC) using recombinant adeno-associated virus (rAAV): *in vitro* and *in vivo* effects of genotoxic agents. J Hepatol 32: 975-985, 2000.
16. Furman PA, McGuirt PV, Keller PM, Fyfe JA and Elion GB: Inhibition by acyclovir of cell growth and DNA synthesis of cells biochemically transformed with herpesvirus genetic information. Virology 102: 420-430, 1980.
17. Cheng YC, Grill SP, Dutschman GE, Nakayama K and Bastow KF: Metabolism of 9-(1,3-dihydroxy-2-propoxymethyl) guanine, a new anti-herpes virus compound, in herpes simplex virus-infected cells. J Biol Chem 258: 12460-12464, 1983.
18. Trask TW, Trask RP, Aguilar-Cordova E, *et al*: Phase I study of adenoviral delivery of the HSV-tk gene and ganciclovir administration in patients with current malignant brain tumors. Mol Ther 1: 195-203, 2000.
19. Hasenburg A, Tong XW, Rojas-Martinez A, *et al*: Thymidine kinase gene therapy with concomitant topotecan chemotherapy for recurrent ovarian cancer. Cancer Gene Ther 7: 839-844, 2000.
20. Sutton MA, Freund CT, Berkman SA, *et al*: *In vivo* adenovirus-mediated suicide gene therapy of orthotopic bladder cancer. Mol Ther 2: 211-217, 2000.
21. Makinen K, Loimas S, Wahlfors J, Alhava E and Janne J: Evaluation of herpes simplex thymidine kinase mediated gene therapy in experimental pancreatic cancer. J Gene Med 2: 361-367, 2000.
22. Kawashita Y, Ohtsuru A, Kaneda Y, *et al*: Regression of hepatocellular carcinoma *in vitro* and *in vivo* by radiosensitizing suicide gene therapy under the inducible and spatial control of radiation. Hum Gene Ther 10: 1509-1519, 1999.
23. Rogulski KR, Wing MS, Paielli DL, Gilbert JD, Kim JH and Freytag SO: Double suicide gene therapy augments the anti-tumor activity of a replication-competent lytic adenovirus through enhanced cytotoxicity and radiosensitization. Hum Gene Ther 11: 67-76, 2000.
24. Kanazawa T, Mizukami H, Okada T, *et al*: Suicide gene therapy using AAV-HSVtk/ganciclovir in combination with irradiation results in regression of human head and neck cancer xenografts in nude mice. Gene Ther 10: 51-58, 2003.
25. Wilkie NM, Clements JB, Boll W, Mantei N, Lonsdale D and Weissmann C: Hybrid plasmids containing an active thymidine kinase gene of Herpes simplex virus 1. Nucleic Acids Res 7: 859-877, 1979.
26. Matsushita T, Elliger S, Elliger C, *et al*: Adeno-associated virus vectors can be efficiently produced without helper virus. Gene Ther 5: 938-945, 1998.
27. Wang JC: DNA topoisomerases. Annu Rev Biochem 65: 635-692, 1996.

28. Qing K, Khuntirat B, Mah C, *et al*: Adeno-associated virus type 2-mediated gene transfer: correlation of tyrosine phosphorylation of the cellular single-stranded D sequence-binding protein with transgene expression in human cells *in vitro* and murine tissues *in vivo*. J Virol 72: 1593-1599, 1998.
29. Sanlioglu S, Duan D and Engelhardt JF: Two independent molecular pathways for recombinant adeno-associated virus genome conversion occur after UV-C and E4orf6 augmentation of transduction. Hum Gene Ther 10: 591-602, 1999.
30. Kunke D, Grimm D, Denger S, *et al*: Preclinical study on gene therapy of cervical carcinoma using adeno-associated virus vectors. Cancer Gene Ther 7: 766-777, 2000.
31. Okada H, Miyamura K, Itoh T, *et al*: Gene therapy against an experimental glioma using adeno-associated virus vectors. Gene Ther 3: 957-964, 1996.
32. Su H, Lu R, Chang JC and Kan YW: Tissue-specific expression of herpes simplex virus thymidine kinase gene delivered by adeno-associated virus inhibits the growth of human hepatocellular carcinoma in athymic mice. Proc Natl Acad Sci USA 94: 13891-13896, 1997.
33. Reid T, Galanis E, Abbruzzese J, *et al*: Intra-arterial administration of a replication-selective adenovirus (dl1520) in patients with colorectal carcinoma metastatic to the liver: a phase I trial. Gene Ther 8: 1618-1626, 2001.
34. Qiao J, Black ME and Caruso M: Enhanced ganciclovir killing and bystander effect of human tumor cells transduced with a retroviral vector carrying a herpes simplex virus thymidine kinase gene mutant. Hum Gene Ther 11: 1569-1576, 2000.
35. Valerie K, Brust D, Farnsworth J, *et al*: Improved radiosensitization of rat glioma cells with adenovirus-expressed mutant herpes simplex virus-thymidine kinase in combination with acyclovir. Cancer Gene Ther 7: 879-884, 2000.

Translocation and cleavage of myocardial dystrophin as a common pathway to advanced heart failure: A scheme for the progression of cardiac dysfunction

Teruhiko Toyo-Oka*†‡§, Tomie Kawada¶, Jumi Nakata*, Han Xie*, Masashi Urabe‖, Fujiko Masui*, Takashi Ebisawa*, Asaki Tezuka*, Kuniaki Iwasawa†‡, Toshiaki Nakajima‡, Yoshio Uehara†, Hiroyuki Kumagai**, Sawa Kostin††, Jutta Schaper††, Mikio Nakazawa‡‡, and Keiya Ozawa‖

*Department of Pathophysiology and Internal Medicine, †Health Service Center, and ‡Department of Cardiovascular Medicine, University of Tokyo, Tokyo 113-0033, Japan; ¶Division of Pharmacy and ‡‡Department of Medical Technology, Niigata University, Niigata 951-8520, Japan; ‖Division of Gene Therapy, Jichi Medical School, Tochigi 329-0498, Japan; **Department of Pharmacology, Gunma University, Maebashi 371-8511, Japan; and ††Department of Experimental Cardiology, Max Planck Institute, Bad Nauheim 61231, Germany

Communicated by Setsuro Ebashi, Okazaki National Research Institutes, Okazaki, Japan, March 25, 2004 (received for review January 24, 2004)

Advanced heart failure (HF) is the leading cause of death in developed countries. The mechanism underlying the progression of cardiac dysfunction needs to be clarified to establish approaches to prevention or treatment. Here, using TO-2 hamsters with hereditary dilated cardiomyopathy, we show age-dependent cleavage and translocation of myocardial dystrophin (Dys) from the sarcolemma (SL) to the myoplasm, increased SL permeability *in situ*, and a close relationship between the loss of Dys and hemodynamic indices. In addition, we observed a surprising correlation between the amount of Dys and the survival rate. Dys disruption is not an epiphenomenon but directly precedes progression to advanced HF, because long-lasting transfer of the missing *δ-SG* gene to degrading cardiomyocytes *in vivo* with biologically nontoxic recombinant adenoassociated virus (rAAV) vector ameliorated all of the pathological features and changed the disease prognosis. Furthermore, acute HF after isoproterenol toxicity and chronic HF after coronary ligation in rats both time-dependently cause Dys disruption in the degrading myocardium. Dys cleavage was also detected in human hearts from patients with dilated cardiomyopathy of unidentified etiology, supporting a scheme consisting of SL instability, Dys cleavage, and translocation of Dys from the SL to the myoplasm, irrespective of an acute or chronic disease course and a hereditary or acquired origin. Hereditary HF may be curable with gene therapy, once the responsible gene is identified and precisely corrected.

Despite the steady progress of pharmaceutical therapy, it is still difficult to completely prevent heart failure (HF) from proceeding to an advanced stage. Cardiac transplantation is the last choice to save the patient at the end stage, and this treatment entails many sociomedical problems. An alternative strategy for therapy is urgently required (1, 2). Primary or secondary degradation of dystrophin (Dys) might be of great significance in determining the cause of HF. Muscular dystrophy results in HF, and poor outcome in patients and animal models is associated with genetic mutations of Dys or the sarcoglycan (SG) complex (1–6). In the present study, we examined the following phenomena: (*i*) the time course of the hemodynamics with biventricular catheterization under stable anesthesia (7) until the TO-2 animals started to show overt HF and cardiac death; (*ii*) *in situ* sarcolemma (SL) stability by double fluoromicroscopy for the entry of an SL-impermeable dye, Evans blue dye (EB), into cardiomyocytes (8) and immunostaining of Dys or δ-SG; (*iii*) Western blotting of Dys and protein quantification; (*iv*) the correlation between limited proteolysis of Dys and hemodynamics; and (*v*) *in vivo* gene transduction in TO-2 hamsters. We also evaluated pathological features in rats with acute and acquired HF due to isoproterenol (Isp) toxicity (9) and in humans with advanced dilated cardiomyopathy (DCM).

Materials and Methods

Experimental Animals, the *rAAV* Vector Gene Construct, and *in Vivo* Gene Delivery. Male F_1B (control) and TO-2 hamster strains were obtained from Bio Breeders (Watertown, MA), and rAAV/lacZ vector alone or a mixture of recombinant adenoassociated virus (rAAV)/lacZ and rAAV/δ-SG was intramurally injected into the cardiac apex of the 5-week-old hamsters (7). pW1, an rAAV plasmid containing lacZ or a 1.2-kb fragment of δ-SG cDNA flanked by inverted terminal repeats of the AAV genome, pHLP19, a helper plasmid with *rep* and *cap* genes, and pladeno-1, a plasmid harboring the adenovirus *E2A*, *E4*, and *VA* genes, were used for rAAV/lacZ or rAAV/δ-SG production. pWSG with a δ-SG expression cassette driven by a cytomegalovirus (CMV) promoter was used for rAAV/δ-SG production (7, 8). Under open chest surgery with constant-volume ventilation, rAAV/lacZ alone or a mixture of rAAV/lacZ and rAAV/δ-SG was intramurally injected into the cardiac apex twice (each injection was 15 μl, for a total of 8.4×10^{10} and 6×10^{10} copies for lacZ and δ-SG, respectively).

Morphological and Immunological Analyses. A polyclonal, site-directed antibody to δ-SG was prepared at a high titer, by using a synthetic peptide with a sequence deduced from the cloned cDNA as a specific epitope (4). Monoclonal antibodies to Dys and to the transgene of lacZ (β-galactosidase) were obtained from NovoCastra (Newcastle, U.K.) and Funakoshi (Tokyo). The density of antibody-specific bands for the rod domain of Dys was measured within a linear intensity range for the applied amount of protein, after Western blotting of whole-heart homogenates, by 5–15% SDS/PAGE. For the Isp study, 10–20% SDS/PAGE was used to detect degradation products of both Dys and δ-SG. To simultaneously monitor Dys disruption, SL fragility *in situ*, and expression of the δ-SG transgene, double fluoromicroscopy was used to detect immunostaining of Dys with a FITC-labeled antibody specific to the rod domain of Dys, the entry of membrane-impermeable EB into cardiomyocytes, and immunostaining of δ-SG with a rhodium isothiocyanate (RITC)-labeled specific antibody by using a Nikon Diaphot or a Leica (Heidelberg, Germany) TCS SL confocal microscope. Where indicated, the Dys immunoproduct in the SL and myoplasm was semiquantified on cardiomyocytes, with or without transduction of δ-SG in the same observation field.

Abbreviations: HF, heart failure; Dys, dystrophin; SG, sarcoglycan; SL, sarcolemma; EB, Evans blue dye; Isp, isoproterenol; DCM, dilated cardiomyopathy; rAAV, recombinant adenoassociated virus; LVP, left ventricular pressure; EDP, end diastolic pressure; CVP, central venous pressure.

§To whom correspondence should be addressed. E-mail: toyooka_3im@hotmail.com.

Table 1. Cardiac hemodynamics with progression of HF

Strain	Age, weeks	LVP, mmHg	dP/dt_{max}, mmHg/sec	dP/dt_{min}, mmHg/sec	EDP, mmHg	CVP, mmHg
F_1B	5	82.9 ± 1.2	4,385 ± 91	−4,503 ± 208	3.1 ± 0.6	1.70 ± 0.53
	15	132.9 ± 5.5†	8,188 ± 743†	−7,188 ± 971†	1.8 ± 1.5	0.78 ± 0.50
	25	132.5 ± 6.9	6,709 ± 188	−6,513 ± 602	1.7 ± 2.7	0.46 ± 0.21
	40	125.1 ± 9.6	7,063 ± 290	−7,180 ± 576	1.6 ± 0.9	−0.62 ± 0.32
TO-2	5	83.0 ± 2.1	4,599 ± 192	−5,175 ± 233*	1.9 ± 0.3*	2.82 ± 0.17*
	15	100.2 ± 4.7*†	4,645 ± 637*	−3,664 ± 378*†	8.8 ± 1.9*†	2.70 ± 0.87*
	25	87.9 ± 8.3*	5,240 ± 388*	−3,171 ± 80*	12.8 ± 1.6*	3.12 ± 0.88*
	40	80.0 ± 2.8*	4,283 ± 97*	−3,120 ± 145*	18.0 ± 1.4*†	9.35 ± 1.35*†

Hemodynamic indices measured under stable anesthesia (7, 8): LVP, its maximum derivative (dP/dt_{max}) and minimum derivative (dP/dt_{min}), EDP, and CVP, in control (F_1B strain) and hereditary DCM (TO-2 strain) hamsters. Each value is shown as the mean ± SE (n = 4–8 hamsters in each group). * and † indicate statistical significance ($P < 0.05$) compared with the F_1B strain and the preceding age, respectively.

Hemodynamic Studies and Statistical Analyses. Peak left ventricular pressure (LVP), left ventricular end diastolic pressure (EDP), its first derivative (dP/dt), and central venous pressure (CVP) were measured under stable anesthesia (7, 8). All values were expressed as the mean ± SE and evaluated by paired Student's t test, ANOVA, and correlation analyses. A P value of <0.05 was considered significant.

Results and Discussion

Progression of DCM to Advanced HF in TO-2 Hamsters. Control F_1B hamsters showed growth-dependent increases in the peak LVP, the maximum rate of LVP (dP/dt_{max}), and the minimum rate of LVP (dP/dt_{min}, Table 1). In contrast, TO-2 hamsters persistently demonstrated systolic failure characterized by reduced LVP, dP/dt_{max}, and blunted dP/dt_{min}. Congestive HF was documented by increased left ventricular EDP and CVP. These signs became aggravated between 25 and 40 weeks of age, when the rate of cardiac death sharply increased (see below). The EDP and CVP reached levels 9.5 and 3.3 times higher, respectively, than those at 5 weeks of age.

Translocation of Dys from the SL to the Myoplasm During DCM Progression. Cardiac samples from TO-2 hamsters revealed time-dependent pathological features at each age (Fig. 1). After 5 weeks, double fluoromicroscopy showed that Dys was neatly arranged on the SL, and EB administered *i.v.* before killing the animals did not enter the myoplasm, indicating that the integrity of the SL was well preserved. After 25 and 40 weeks, the Dys on the SL became blurred, and some cardiomyocytes demonstrated a shift of Dys from the SL to the myoplasm. We refer to this phenomenon as "translocation" of Dys. These cardiomyocytes matched exactly with cells that took up EB (within ovals), denoting that the SL of the translocated cells leaked the exogenously applied dye.

Cleavage of Dys in Hamster Heart and in the Hearts of Humans with DCM. Western blotting of the myocardial homogenate with an antibody specific to the rod domain of Dys showed characteristic features (Fig. 2*a Left*). Normal hearts at 5 weeks of age showed a band at 430 kDa corresponding to normal Dys, and the staining intensity was preserved up to 40 weeks of age. Striking differences were observed in TO-2 hamsters, although at 5 and 15 weeks of age the staining pattern did not differ from that of the F_1B heart. However, at 25 weeks of age, extra bands were detected between 60 and 200 kDa (Fig. 2*a Left*), and the intensity of the Dys 430-kDa band started to decline. The intensity of this band was markedly reduced between 25 and 40 weeks of age, whereas the intensity of the 60-kDa band increased, mirroring the Dys band (Fig. 2*b*). The period of significant Dys cleavage matched exactly the periods when Dys translocation became

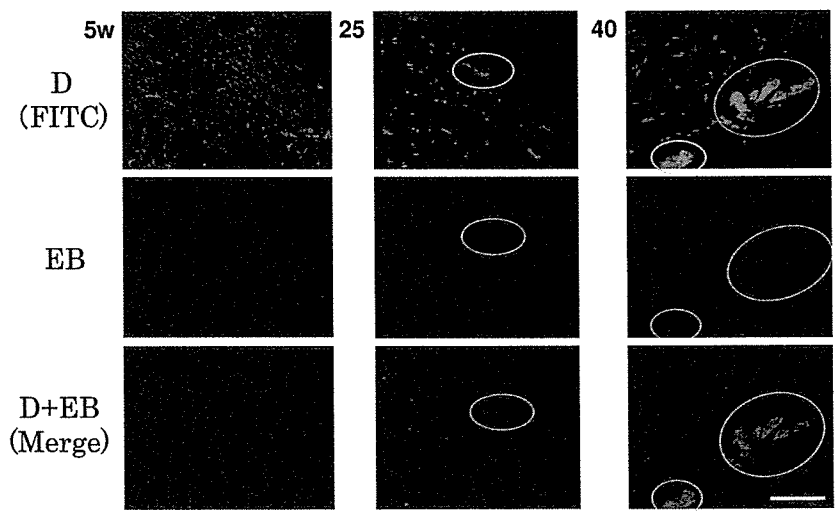

Fig. 1. Age-dependent translocation of Dys and increased permeability of the SL during HF progression in TO-2 hamsters. Double fluoromicroscopy for detection of a FITC-labeled antibody to the rod domain of Dys and entry of membrane-impermeable, fluorescent EB, at 5, 25, and 40 weeks of age (w). Cardiomyocytes demonstrating a shift of Dys from the SL to the myoplasm are shown in ovals. (Bar = 40 μm.)

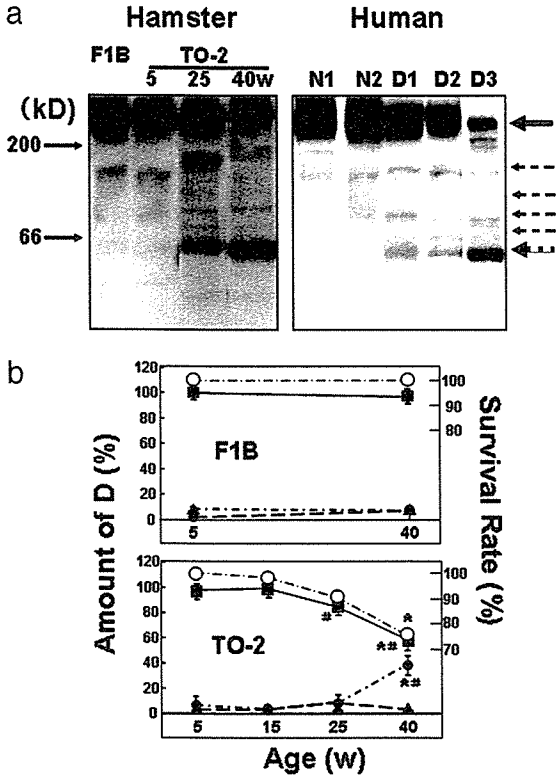

Fig. 2. Cleavage and reduction of cardiac Dys during DCM progression in hamsters and humans. (*a Left*) Control (F_1B strain) or DCM (TO-2 strain) hamsters at 5, 25, and 40 weeks of age (w). (*a Right*) Normal human myocardium (N1 and N2) and DCM hearts (D1, D2, and D3) at the time of cardiac transplantation. A solid arrow at 430 kDa and several dotted arrows denote the original Dys and its degradation products, respectively, after 5–20% SDS/PAGE of whole-heart homogenates. (*b*) Time course of the survival rate of control (F_1B; *Upper*) or DCM (TO-2; *Lower*) hamsters (○) and the density of immunoreactive bands specific to the rod domain of Dys at 430 (■), 60 (●) or 160 (▲) kDa. * and # indicate a significant difference, compared with the control F_1B strain and the preceding age, respectively.

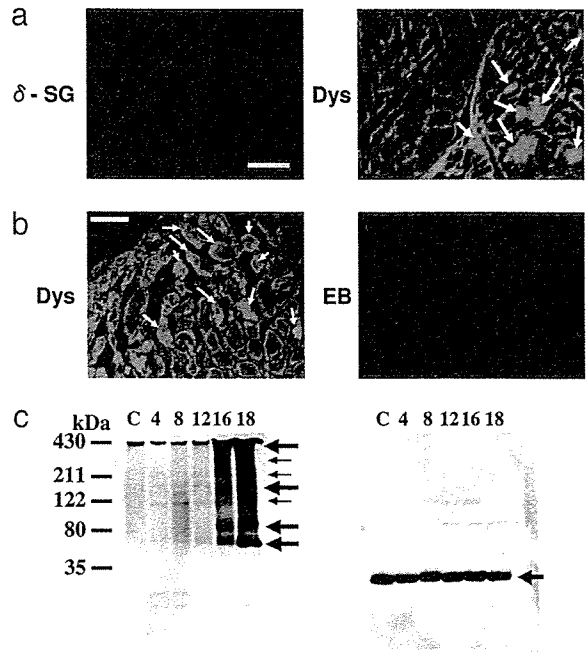

Fig. 3. (*a*) Double immunostaining of δ-SG (rhodamine isothiocyanate) and Dys (FITC) of TO-2 hamster hearts 35 weeks after local δ-SG gene transfection *in vivo* (8). Arrows indicate cardiomyocytes where dystrophin was translocated from the SL to the myoplasm. (Bar = 40 μm.) (*b*) Assessment of Dys translocation (FITC) and SL fragility *in situ* (EB entry) 16 h after the administration of Isp at a high dose (10 mg/kg i.p.) in Wistar rats (15). Arrows indicate cardiomyocytes where dystrophin was translocated from the SL to the myoplasm. (Bar = 40 μm.) (*c*) Western blotting of Dys (*Left*) and δ-SG (*Right*) from the same rat heart homogenate sample after gradient 10–15% SDS/PAGE of the control (C) and 4, 8, 12, 16 and 18 h after Isp treatment. Arrows indicate uncleaved Dys (430 kDa) and Dys degradation products (*Left*) or δ-SG (*Right*).

evident (Fig. 1) and when the animals started to die of congestive HF (ref. 8 and Fig. 2*b*). The intensity of the faint 160-kDa band did not change throughout the study and appeared to be unrelated to the progression of HF.

Similar cleavage of Dys was confirmed in hearts from patients with DCM of unidentified etiology who had undergone cardiac transplantation (Fig. 2*a Right*). The topological shift of Dys was also documented in samples of advanced stage DCM (unpublished data). Accordingly, the translocation was common to both animal models and patients with DCM. Other antibodies to the C or N terminus of Dys did not clearly recognize the cleavage product (data not shown). At present, we do not know the reason for this discrepancy in human cases of advanced HF showing selective cleavage of Dys at the N terminus (10).

Relationship of Dys Cleavage to Hemodynamics and the Lifespan of Hamsters. Surprisingly, the amount of Dys or its 60-kDa-band degradation product in TO-2 animals very closely correlated with the hemodynamic indices that characterize the progression of HF. The Dys amount was positively correlated with the systolic index [peak LVP, coefficient of regression (r) = 0.998 and $P < 0.0004$], and negatively correlated with the diastolic parameters (EDP, $r = 0.996$ and $P < 0.0005$; CVP, $r = 0.954$ and $P < 0.002$). The intensity of the 60-kDa band showed a clear negative correlation with the LVP ($r = 0.961$, $P < 0.002$) and a positive correlation with the EDP ($r = 0.954$, $P < 0.002$) and CVP ($r = 0.996$, $P < 0.0005$). These highly significant regression coefficients for correlation of the amount of Dys with systolic or diastolic performance support a tentative role for Dys in transmitting an effect through the actin–myosin linkage to the extracellular matrix. It is also noteworthy that no correlation was found between the amounts of Dys or the 60-kDa band and the dP/dt_{max} or dP/dt_{min} value (data not shown), both of which are regulated by Ca^{2+} handling (11) and the energetics of cardiac muscle cells (12). It should be emphasized that a distinct relationship was found between the amount of Dys or the 60-kDa band and the survival rate of the TO-2 animals over time (Fig. 2*b Lower*). It is possible that these immunological and hemodynamic data could be biased, because ≈30% of the TO-2 hamsters died of HF (Fig. 2*b Lower*), and we could only use the survivors in the analysis.

Effect of Long-Lasting Gene Therapy on Dys Localization. The final evidence that the disruption of Dys is not an epiphenomenon in HF but is actually caused by a loss of δ-SG is provided by the double immunostaining of Dys and δ-SG in TO-2 hearts with or without local gene transfection *in vivo* (Fig. 3*a*). In control F_1B hearts, both proteins were equally expressed on the SL (data not shown). In contrast, the TO-2 heart did not express δ-SG (13). As described above (Fig. 1), Dys staining became blurred with age, and some cardiomyocytes revealed Dys translocation (14). Gene delivery of normal δ-SG *in vivo*, by means of a nonpathogenic and long-lasting rAAV vector (7, 8), was used to locally express the δ-SG transgene, and this gene therapy completely ameliorated Dys translocation in the same cardiomyocytes for up to 35 weeks (Fig. 3*a Left*). In contrast, nontransfected cells

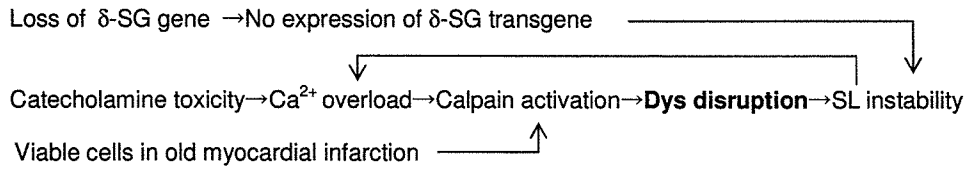

Scheme 1. Pathways for the progression of HF to an advanced stage.

showed translocation of Dys in the same sample (indicated by arrows in Fig. 3*a Right*). This finding specifically eliminates the possibility that Dys disruption resulted from the parallel development of HF, because Dys translocation was restricted to cardiomyocytes that did not express the δ-SG transgene. Furthermore, the amount of Dys estimated *in situ* by densitometry of immunofluoromicroscopic images in cardiomyocytes indicated a 1.22 ± 0.13 fold ($P < 0.01$) preferential localization of Dys on the SL of δ-SG-transfected cells ($n = 70$ cells per group).

Effect of Isp on SL Permeability, and Shift and Cleavage of Dys and δ-SG. A toxic dose of Isp (10 mg/kg i.p.) causes acute HF and morphological deterioration in normal rats (9). Pathological examination has shown time-dependent degradation of Dys and apoptosis of cardiomyocytes from 4 to 18 h after Isp was administered (15). Confocal microscopy of cardiomyocytes in the same observation field showed translocation of Dys (indicated by arrows in Fig. 3*b Left*) and entry of the SL-impermeable EB into the myoplasm of cardiac muscle cells. The shift of Dys was selectively detected 16 h after Isp treatment only in cardiomyocytes where EB had entered the myoplasm (Fig. 3*b Right*). Western blotting revealed time-dependent cleavage of Dys, showing degradation fragments between 60 and 200 kDa (Fig. 3*c Left*). In contrast, δ-SG was not hydrolyzed at all (Fig. 3*c Right*). Immunohistology confirmed that δ-SG did not shift from the SL but remained localized on the SL (data not shown). The effect of high-dose Isp, a β-adrenergic agonist, was similar to that observed in a DCM mouse with a protein kinase A knock-in gene (16). To verify the therapeutic effect of gene therapy in a β-adrenergic agonist/protein kinase A/phospholamban system, the pharmacological action (17, 18) and the disease prognosis need to be precisely examined, because an improvement in hemodynamics does not always prolong the lifespan of the animal (19).

The limited hydrolysis of Dys, common to the models of acute and chronic diseases in the present study, suggests a role for calpain, because cardiomyocytes contain an appreciable amount of this protein (20), and intracellular Ca^{2+} handling is modified in failing hearts (21, 22). Neither a specific inhibitor for calpain nor a calpain knockout animal is currently available to test this hypothesis. β-Adrenergic agonists induce Ca^{2+} overload in cardiomyocytes by increasing Ca^{2+} uptake (23). In addition, Dys and α-, β-, and γ-SG, but not δ-SG, are hydrolyzed by the endogenous protease (24) or isolated calpain *in vitro* (25, 26). The preferential breakdown of these proteins, but not δ-SG, in three HF models, i.e., TO-2 hamster hearts (13), Isp-treated rat hearts (Fig. 3*b*), and viable cells at the end stage of myocardial infarction (26), might be accompanied by substantially enhanced activity of *m*-calpain over its endogenous inhibitor, calpastatin. The expression of *m*-calpain in TO-2 hearts markedly exceeded that of calpastatin during the progression of HF (data not shown). These results may imply that the balance between calpain and calpastatin will shift in a calpain-dominant manner. Furthermore, dot hybridization analyses revealed no increment of mRNA of each DAP component under these HF conditions, suggesting that compensatory biosynthesis did not occur in the case of DAP.

A Scheme for the Progression of HF to an Advanced Stage. The clinical link between excess stimulation with catecholamines and myocardial damage has been confirmed by the therapeutic success of β-adrenergic antagonists in TO-2 hamsters (27) and humans (28, 29). The cleavage of Dys has also been documented after enterovirus infection, resulting in DCM-like HF (30). These pathological findings present a paradigm in which cardioselective cleavage of Dys may lead to progression of HF to an advanced stage (Scheme 1). Scheme 1 does not exclude the involvement of a protease cascade, as seen through the activation of a calpain-like homologue in neuronal degeneration in *Caenorhabditis elegans* (31), or involvement of the ubiquitin/proteasome system (32) in the loss of Dys. More definite evidence is required to precisely determine the causative factor(s). This common pathological process, irrespective of the hereditary or acquired origin and the chronic or acute course of the disease, suggests a strategy for the treatment of advanced HF through interruption of the vicious circle by either gene therapy or drug treatment.

We thank Dr. John R. Solaro (Department of Physiology and Biophysics, University of Illinois, Chicago) for discussion of the results and Dr. Y. Niwa and K. Kurosawa (Department of Pathophysiology, University of Tokyo) for experimental and secretarial assistance. This work was supported by Ministry of Education, Culture, and Science Grant A2 142070333 and by the Ministry of Welfare and Labor, Japan, the Mitsubishi Research Foundation, and the Motor Vehicle Foundation.

1. Cox, G. F. & Kunkel, L. M. (1997) *Curr. Opin. Cardiol.* **12,** 329–343.
2. Seidman, J. G. & Seidman, C. (2001) *Cell* **104,** 557–567.
3. Durbeej, M. & Campbell, K. P. (2002) *Curr. Opin. Genet. Dev.* **12,** 349–361.
4. Sakamoto, A., Ono, K., Abe, M., Jasmin, G., Eki, T., Murakami, Y., Masaki, T., Toyo-oka, T. & Hanaoka, F. (1997) *Proc. Natl. Acad. Sci. USA* **94,** 13873–13878.
5. Nigro, V., Okazaki, Y., Belsito, A., Piluso, G., Matsuda, Y., Politano, L., Nigro, G., Ventura, C., Abbondanza, C., Molinari, A. M., *et al.* (1997) *Hum. Mol. Genet.* **6,** 601–607.
6. Tsubata, S., Bowles, K. R., Vatta, M., Zintz, C., Titus, J., Muhonen, L., Bowles, N. E. & Towbin, J. A. (2000) *J. Clin. Invest.* **106,** 655–662.
7. Kawada, T., Sakamoto, A., Nakazawa, M., Urabe, M., Masuda, F., Hemmi, C., Wang, Y., Shin, W. S., Nakatsuru, Y., Sato, H., *et al.* (2001) *Biochem. Biophys. Res. Commun.* **284,** 431–435.
8. Kawada, T., Nakazawa, M., Nakauchi, S., Yamazaki, K., Shimamoto, R., Urabe, M., Nakata, J., Masui, F., Nakajima, T., Suzuki, J., *et al.* (2002) *Proc. Natl. Acad. Sci. USA* **99,** 901–906.
9. Kahn, D. S., Rona, G. & Chappel, C. I. (1969) *Ann. N.Y. Acad. Sci.* **156,** 285–293.
10. Vatta, M., Stetson, S. J., Perez-Verdia, A., Entman, M. L., Noon, G. P., Torre-Amione, G., Bowles, N. E. & Towbin, J. A. (2002) *Lancet* **359,** 936–941.
11. Ebashi, S., Nonomura, Y., Toyo-oka, T. & Katayama, E. (1976) *Symp. Soc. Exp. Biol.* **30,** 349–360.
12. Toyo-oka, T., Nagayama, K., Suzuki, J. & Sugimoto, T. (1992) *Circulation* **86,** 295–301.
13. Kawada, T., Nakatsuru, Y., Sakamoto, A., Koizumi, T., Shin, W. S., Okai-Matsuo, Y., Suzuki, J., Uehara, Y., Nakazawa, M., Satoh, H., *et al.* (1999) *FEBS Lett.* **458,** 405–408.
14. Kawada, T., Hemmi, C., Fukuda, S., Iwasawa, K., Tezuka, A., Nakazawa, M., Sato, H. & Toyo-oka, T. (2004) *Exp. Clin. Cardiol.* **8,** in press.
15. Xi, H., Shin, W. S., Suzuki, J., Nakajima, T., Kawada, T., Uehara, Y., Nakazawa, M. & Toyo-oka, T. (2000) *J. Cardiovasc. Pharmacol.* **36,** Suppl. 2, S25–S29.
16. Antos, C. L., Frey, N., Marx, S. O., Reiken, S., Gaburjakova, M., Richardson, J. A., Marks, A. R. & Olson, E. N. (2001) *Circ. Res.* **89,** 997–1004.

THE JOURNAL OF GENE MEDICINE
J Gene Med 2004; 6: 22–31.
Published online 5 November 2003 in Wiley InterScience (www.interscience.wiley.com). **DOI:** 10.1002/jgm.467

RESEARCH ARTICLE

In vivo expansion of gene-modified hematopoietic cells by a novel selective amplifier gene utilizing the erythropoietin receptor as a molecular switch

Takeyuki Nagashima[1]
Yasuji Ueda[1]*
Yutaka Hanazono[2]
Akihiro Kume[3]
Hiroaki Shibata[4]
Naohide Ageyama[4]
Keiji Terao[4]
Keiya Ozawa[3]
Mamoru Hasegawa[1]

[1]*DNAVEC Research Inc., Ibaraki 305-0856, Japan*

[2]*Division of Regenerative Medicine, Center for Molecular Medicine, Jichi Medical School, Tochigi 329-0498, Japan*

[3]*Division of Genetic Therapeutics, Center for Molecular Medicine, Jichi Medical School, Tochigi 329-0498, Japan*

[4]*Tsukuba Primate Center, National Institute of Infectious Diseases, Ibaraki 305-0843, Japan*

*Correspondence to: Yasuji Ueda, DNAVEC Research Inc., Ibaraki 305-0856, Japan.
E-mail: yueda@dnavec.co.jp

Received: 22 April 2003
Revised: 21 July 2003
Accepted: 21 July 2003

Abstract

Background *In vivo* expansion of gene-modified cells would be a promising approach in the field of hematopoietic stem cell gene therapy. To this end, we previously developed a selective amplifier gene (SAG), a chimeric gene encoding the granulocyte colony-stimulating factor (G-CSF) receptor (GCR), as a growth-signal generator and the hormone-binding domain of the steroid receptor as a molecular switch. We have already reported that hematopoietic cells retrovirally transduced with the SAG can be expanded in a steroid-dependent manner *in vitro* and *in vivo* in mice and nonhuman primates. In this study, we have developed a new-generation SAG, in which the erythropoietin (EPO) receptor (EPOR) is utilized instead of the steroid receptor as a molecular switch.

Methods Two EPO-driven SAGs were constructed, EPORGCR and EPORMpl, containing the GCR and c-Mpl as a signal generator, respectively. First, to compare the steroid-driven and EPO-driven SAGs, Ba/F3 cells were transduced with these SAGs. Next, to examine whether GCR or c-Mpl is the more suitable signal generator of the EPO-driven SAG, human cord blood $CD34^+$ cells were transduced with the two EPO-driven SAGs (EPORMpl and EPORGCR). Finally, we examined the *in vivo* efficacy of EPORMpl in mice. Irradiated mice were transplanted with EPORMpl-transduced bone marrow cells followed by administration of EPO.

Results The EPO-driven SAGs were shown to induce more rapid and potent proliferation of Ba/F3 cells than the steroid-driven SAGs. The EPORMpl induced more efficient EPO-dependent proliferation of the human cord blood $CD34^+$ cells than the EPORGCR in terms of total $CD34^+$ cell, c-Kit^+ cell, and clonogenic progenitor cell (CFU-C) numbers. In the transplanted mice the transduced peripheral blood cells significantly increased in response to EPO.

Conclusions The new-generation SAGs, especially EPORMpl, are able to efficiently confer an EPO-dependent growth advantage on transduced hematopoietic cells *in vitro* and *in vivo* in mice.

Keywords hematopoietic stem cells; gene therapy; $CD34^+$ cells; selective amplifier gene; *in vivo* expansion; retroviral vector

Introduction

One of the major obstacles associated with hematopoietic stem cell (HSC) gene therapy is the low efficiency of gene transfer into human HSCs with retroviral vectors [1]. The ability to positively select cells containing potentially therapeutic genes *in vivo* would represent an important tool for the clinical application of HSC gene therapy. A promising strategy of *in vivo* positive selection of transduced cells is to confer a direct proliferation advantage on gene-modified cells relative to their untransduced counterparts. We developed a chimeric gene designated 'selective amplifier gene' (SAG) which encodes a chimeric receptor between the granulocyte colony-stimulating factor (G-CSF) receptor (GCR) and the hormone-binding domain of the estrogen or tamoxifen receptor. The GCR moiety is a growth-signal generator and the estrogen receptor (ER) moiety is a molecular switch to regulate (turn on or off) the growth signal generated from the GCR. We previously showed that hematopoietic cells transduced with the SAG can be selectively expanded in an estrogen- or tamoxifen-dependent manner *in vitro* [2–5] and *in vivo* in mice and nonhuman primates [6,7]. In nonhuman primates, however, some animals that received the SAG did not show an increase in transduced cells in response to estrogen or tamoxifen, suggesting that the SAG was not potent enough to achieve *in vivo* expansion in all animals [7].

The utilization of the steroid receptor as a molecular switch may have attenuated the potency of the SAG. The estrogen-mediated dimerization of the chimeric molecule may be less efficient than the natural ligand (G-CSF)-mediated dimerization. In fact, the fusion protein between the GCR and estrogen receptor responds to G-CSF more efficiently than to estrogen [2]. To rectify this problem, we utilized the erythropoietin receptor (EPOR) instead of the steroid receptor as a molecular switch. Since the EPOR is a member of the cytokine receptor superfamily [8], the fusion proteins between the EPOR and other cytokine receptors such as the GCR should be more stable and compatible than the prototype fusion protein. In addition, the EPOR is not expressed on immature hematopoietic cells and thus can be used as a selective switch for these cells [9]. Of note, recombinant human erythropoietin (EPO) has already been used widely in clinical application and can be administered repeatedly to human subjects without serious adverse effects [10,11].

On the other hand, as a growth-signal generator, we tried to use the thrombopoietin (TPO) receptor, c-Mpl, in addition to the GCR. It has been reported that c-Mpl is expressed on very immature hematopoietic cells and that TPO actually stimulates the growth of these cells [12–15]. In fact, the cytoplasmic fragment of c-Mpl has already been used for the purpose of cell expansion [5,16]. The intracellular signal from c-Mpl may thus be more appropriate than that from the GCR for expansion of hematopoietic stem/progenitor cells. In the present study, we examined the efficacy of these new generation SAGs *in vitro* and *in vivo* in mice.

Materials and methods

Cell lines

Ba/F3 cells were maintained in Dulbecco's modified Eagle's medium (DMEM; Gibco-BRL, Grand Island, NY, USA) supplemented with 10% fetal bovine serum (FBS; Gibco-BRL), 1% penicillin/streptomycin (Gibco-BRL), and 1 ng/ml recombinant mouse IL-3 (rmIL-3; Gibco-BRL). The ecotropic packaging cell line BOSC23 [17] and human embryonic kidney 293T cells were maintained in DMEM containing 10% FBS and 1% penicillin/streptomycin.

Plasmid construction

The wild-type human erythropoietin receptor (EPORwt) cDNA was obtained from pCEP4-EPOR (kindly provided by Dr. R. Kralovics, University of Alabama, USA) [18]. The fragment containing the murine phosphoglycerate kinase (pgk) promoter and neomycin phosphotransferase gene (neo) (EcoRI-BamHI) in the retroviral plasmid pMSCV2.2 (kindly provided by Dr. R. G. Hawley, University of Toronto, Canada) [19] was replaced by the EPORwt cDNA (EcoRI-BamHI) to construct pMSCV-EPORwt.

pMSCV-EPORGCR and pMSCV-EPORMpl were constructed as follows. The cytoplasmic region of murine G-CSF receptor (GCR) cDNA was obtained by PCR using pMSCV-ΔY703FGCRER as a template [3] with the primer pair 5′-AAG GAT CCA AAC GCA GAG GAA AGA AGA CT-3′ and 5′-AAG TCG ACC TAG AAA CCC CCT TGT TC-3′. The cDNA coding to the cytoplasmic region of human TPO receptor (c-Mpl) was obtained by PCR using pcDNA3.1-c-Mpl (provided by Dr. M. Takatoku, Jichi Medical School, Tochigi, Japan) [20] as a template with the primer pair 5′-AAG GAT CCA GGT GGC AGT TTC CTG CA-3′ and 5′-CGG TCG ACT CAA GGC TGC TGC CAA TA-3′. The fragment containing the extracellular plus transmembrane region of the human EPOR cDNA was obtained by PCR using pCEP4-EPOR as a template with the primer pair 5′-CTC GGC CGG CAA CGG CGC AGG GA-3′ and 5′-AAG GAT CCC AGC AGC GCG AGC ACG GT-3′. The fragment containing the extracellular plus transmembrane region of human EPOR cDNA and the fragment containing the cytoplasmic region of murine GCR or human c-Mpl were cloned into the EcoRI-SalI site of pBluescript SK (pSK; Stratagene, La Jolla, CA, USA) to construct pSK-EPOGCR or pSK-EPOMpl, respectively. The pgk promoter/neo cassette (EcoR-SalI) in pMSCV was replaced by the EcoRI-SalI fragment containing the EPORGCR or EPORMpl cDNA each from pSK-EPORGCR or pSK-EPORMpl, respectively. The resultant construct was designated as pMSCV-EPORGCR or pMSCV-EPORMpl, respectively.

pMSCV-EPORwt-ires-mitoEYFP, pMSCV-EPORGCR-ires-mitoEYFP, and pMSCV-EPORMpl-ires-mitoEYFP were

constructed as follows. The internal ribosome entry site (ires) sequence derived from pIRES-EGFP (Clontech, Palo Alto, CA, USA) and the mitoEYFP cDNA derived from pEYFP-Mito (Clontech) were inserted into the PstI-BamHI site and the SpeI-NotI site of pSK, respectively. The resultant plasmid was pSK-ires-mitoEYFP. The mitEYFP cDNA encodes the enhanced yellow fluorescent protein (enhanced YFP, EYFP) linked to a mitochondria localization signal sequence so that EYFP is sequestered inside the mitochondria, thus circumventing the presumed toxicity of YFP [21]. The blunted fragment encoding the ires-mitoEYFP cDNA was ligated into the ClaI blunted site of pMSCV-EPORwt, pMSCV-EPORGCR, and pMSCV-EPORMpl to obtain pMSCV-EPORwt-ires-mitoEYFP, pMSCV-EPORGCR-ires-mitoEYFP, and pMSCV-EPORMpl-ires-mitoEYFP, respectively. The final plasmids were certified as correct by sequence analysis.

Retroviral vectors

To obtain ecotropic retroviral vectors, BOSC23 cells were transfected with mouse stem cell virus (MSCV)-based retroviral plasmids (derivatives from pMSCV, see above) using Lipofectamine Plus (Invitrogen, San Diego, CA, USA) according to the manufacturer's protocol and the supernatants containing the ecotropic retroviral vectors were harvested 48–72 h post-transfection. The titers were 1×10^6/ml as assessed by RNA dot-blot. To obtain amphotropic retroviral vectors, 293T cells were transfected with MSCV-based retroviral plasmids along with pCL-Ampho (Imgemex, San Diego, CA, USA) using Lipofectamine Plus and the supernatants containing the amphotropic retroviral vectors were harvested 48–72 h post-transfection. The titers were 1×10^6/ml as assessed by RNA dot-blot.

Retroviral transduction and culture

Ba/F3 cells were suspended in 1 ml retroviral supernatant containing 10 ng/ml rmIL-3 at a density of 1×10^5 cells/ml, and transferred to 12-well plates coated with 20 μg/cm^2 of RetroNectin (Takara Bio, Shiga, Japan) [22]. The cells were incubated at 37 °C in a humidified atmosphere of 5% CO_2 in air for 24 h. During this period, culture medium was replaced by fresh viral supernatant twice (every 12 h). After retroviral infection, YFP-positive cells were isolated using an EPICS ELITE cell sorter (Coulter, Miami, FL, USA). The purity of sorted YFP-positive cells was greater than 98%. The sorted Ba/F3 cells were subjected to further liquid culture (described above) or cell proliferation assays (see below).

Human cord blood CD34$^+$ cells (BioWhittaker, Walkersville, MD, USA) were thawed and placed in 12-well plates coated with 20 μg/cm^2 of RetroNectin and cultured for 24 h at 37 °C with 5% CO_2 in Iscove's modified Dulbecco's medium (IMDM; Gibco-BRL) supplemented with 10% FBS (Hyclone, Logan, UT, USA), 50 ng/ml recombinant human interleukin 6 (rhIL-6; Ajinomoto, Osaka, Japan), 100 ng/ml recombinant human stem cell factor (rhSCF; Biosource, Camarillo, CA, USA), 100 ng/ml recombinant human Flt-3 ligand (Research Diagnostic, Flanders, NJ, USA), and 100 ng/ml recombinant human thrombopoietin (rhTPO; Kirin, Tokyo, Japan). The cells were then resuspended in 1 ml viral supernatant containing the same cytokines as described above at a starting density of 1×10^5 cells/ml. During the transduction period (48 h), culture medium was replaced by fresh viral supernatant four times (every 12 h). After retroviral transduction, human cord blood CD34$^+$ cells were washed twice and cultured in IMDM medium containing 10% FBS (Hyclone) and 1% penicillin/streptomycin in the presence of 10 ng/ml recombinant human EPO (rhEPO; Roche Diagnostics, Mannheim, Germany) in a 37 °C 5% CO_2 incubator. The cells were subjected to flow cytometry or colony assay (see below) on indicated days.

Cell proliferation assay

Ba/F3 proliferation assay was performed using the CellTier 96 Aqueous One Solution cell proliferation assay (Promega, Madison, WI, USA) according to the manufacturer's instructions. In brief, 20 μl MTS (3-[4,5-dimethylthiazol-2-yl]-5-[3-carboxymethoxyphenyl]-2-[4-sulfophenyl]-2*H*-tetrazolium)-labeling mixture was added to each well of 96-well dishes containing cells to be assayed. Following incubation at 37 °C for 2 h, the spectrophotometric absorbance was measured at wavelengths of 490 and 650 nm. A_{490}-A_{650} values were used to determine Ba/F3 cell proliferation. Experiments were conducted in triplicate.

Flow cytometry

Human cord blood CD34$^+$ cells were washed and resuspended in CellWASH (Becton Dickinson, San Jose, CA, USA). The cells were then incubated with phycoerythrin (PE)-labeled anti-c-Kit (Nichirei, Tokyo, Japan), PE-labeled anti-glycophorin A (Nichirei), PE-labeled anti-CD41 (Nichirei), or PE-labeled anti-CD15 (Immunotech, Marseille, France) at 4 °C for 30 min. The cells were washed once and subjected to a FACSCalibur (Becton Dickinson) using excitation at 488 nm. Untransduced cells served as negative controls.

For mouse blood samples, blood cells were suspended in ACK lysis buffer (155 mM NH_4Cl, 10 mM $KHCO_3$, and 0.1 mM EDTA; Wako, Osaka, Japan) to dissolve red blood cells. The cells were washed once and subjected to a FACSCalibur (Becton Dickinson) using excitation at 488 nm.

Colony assay and PCR

Human cord blood CD34$^+$ cells were plated in 35-mm dishes with α-minimum essential medium (Gibco-BRL)

containing 1.2% methylcellulose (Shinetsu Kagaku, Tokyo, Japan) supplemented with 20% FBS (Intergen, Purchase, NY, USA) and 1% bovine serum albumin (Sigma, St. Louis, MO, USA) in the presence of 100 ng/ml rhSCF, 100 ng/ml rhIL-6, and 100 ng/ml recombinant human interleukin 3 (rhIL-3; PeproTech, London, UK), or in the presence of 20 ng/ml of rhEPO alone. After incubation for 14 days at 37 °C in a humidified atmosphere of 5% CO_2 in air, colonies were scored under an inverted microscope. The experiments were performed in triplicate.

Colonies in methylcellulose culture were plucked up under an inverted microscope, suspended in 50 µl of distilled water, and digested with 20 µg/ml proteinase K (Takara) at 55 °C for 1 h followed by incubation at 99 °C for 10 min. PCR was performed to amplify the 351-bp sequence using the EYFP sense primer (5′-CGT CCA GGA GCG CAC CAT CTT C-3′) and antisense primer (5′-AGT CCG CCC TGA GCA AAG ACC-3′). To certify the initial DNA amounts, the β-actin genomic DNA fragment was simultaneously amplified using the sense primer (5′-CAT TGT CAT GGA CTC TGG CGA CGG-3′) and antisense primer (5′-CAT CTC CTG CTC GAA GTC TAG GGC-3′). Amplification conditions were 95 °C for 1min, 55 °C for 30 s, and 72 °C for 30 s with 35 cycles.

Mouse transplantation

Eight-week-old C57Bl/6 mice (Charles River Japan, Yokohama, Japan) intraperitoneally received 150 µg/kg 5-fluorouracil (Sigma). Forty-eight hours after injection, bone marrow cells were harvested from the femora of each mouse. Cells were cultured in IMDM (Gibco-BRL) containing 20% FBS (Hyclone) and 20 ng/ml rhIL-6 and 100 ng/ml recombinant rat SCF (provided by Amgen) for 48 h. The cells were then placed in 6-well plates coated with 20 µg/cm^2 of RetroNectin and resuspended in IMDM supplemented with 10% FBS (Hyclone) and the aforementioned cytokines at a starting density of 5×10^5 cells/ml. During the transduction period (48 h), culture medium was replaced by fresh viral supernatant four times (every 12 h). The cells were harvested after a total of 96 h (4 days) in culture, washed with PBS three times, and injected into 8-week-old female C57/Bl6 mice that had been irradiated with 800 cGy. After transplantation, some mice received recombinant mouse EPO (rmEPO; 200 IU/kg, Roche Diagnostics) in a total volume of 100 µl via the tail vein three times a week. To avoid development of anemia after drawing blood from the transplanted mice, blood was transfused into the mice via the tail vein at the time of blood drawing. The blood for transfusion was drawn from donor C57/Bl6 mice and pooled. It was irradiated with 20 Gy and diluted with physiological salt solution prior to transfusion. Peripheral blood mononuclear cells of the recipient mice were analyzed for EYFP expression by flow cytometry.

Results

A new generation SAG

The structure of the SAGs is shown in Figure 1. The prototype SAG (steroid-driven SAG) is a chimeric gene encoding the G-CSF receptor (GCR) and the estrogen receptor hormone-binding domain. In the GCR, the ligand (G-CSF)-binding domain was deleted to remove the responsiveness to endogenous G-CSF [2]. The tyrosine residue at the 703rd amino acid in the GCR was replaced by phenylalanine to hamper the differentiation signal [3]. In addition, another mutation (G525R) was introduced into the estrogen receptor hormone-binding domain to evade the responsiveness to endogenous estrogen without impairing the responsiveness to synthetic hormones such as tamoxifen [4]. In this study, we constructed a new generation SAG, in which the erythropoietin (EPO) receptor (EPOR) is utilized instead of the estrogen or tamoxifen receptor as a molecular switch. Two types of EPO-driven SAG were constructed, EPORGCR and EPORMpl, containing the GCR gene and the thrombopoietin (TPO)

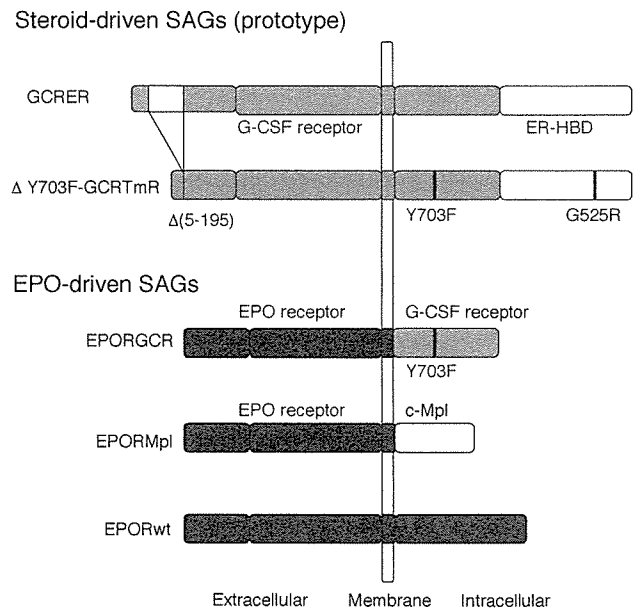

Figure 1. The structure of SAGs. The GCRER is a prototype of the selective amplifier gene (SAG), a chimeric gene encoding the G-CSF receptor (GCR) as a growth-signal generator and the estrogen receptor hormone-binding domain (ER-HBD) as a molecular switch. In ΔY703F-GCRTmR, the G-CSF-binding domain was deleted from the GCR gene to abolish responsiveness to endogenous G-CSF, a point mutation (Y703F) was introduced into the GCR moiety to disrupt the differentiation signal generated by the GCR, and another point mutation (G525R) was introduced into the ER-HBD moiety to evade responsiveness to endogenous estrogen without impairing responsiveness to a synthetic hormone tamoxifen. In the new SAG, the erythropoietin (EPO) receptor (EPOR) was utilized instead of the estrogen or tamoxifen receptor as a molecular switch. To construct it, the intracellular domain of the wild-type EPOR (EPORwt) gene was replaced by that of the GCR or thrombopoietin receptor (c-Mpl) gene as a growth-signal generator

receptor (c-Mpl) gene, respectively, as a growth-signal generator.

In vitro effects of the EPO-driven SAG on Ba/F3

Bicistronic retroviral vectors were generated which express the EPO-driven SAG or wild-type EPOR (EPORwt) gene as the first cistron and the EYFP gene as the second cistron. The vectors were infected into Ba/F3 cells. Ba/F3 is a mouse pro-B cell line and the cells require IL-3 for growth. YFP-positive cells were isolated (>98% purity) and stimulated by rhEPO at various concentrations (Figure 2A). All the cells acquired the ability of EPO-dependent growth and were able to proliferate even in the absence of IL-3. Ba/F3 cells expressing either EPORwt, EPORGCR, or EPORMpl reached the maximum growth levels by adding 1–100 ng/ml EPO (Figure 2A). Endogenous EPO will not induce a significant proliferative response of the cells, since the physiological range of serum EPO concentrations is below 0.1 ng/ml.

We compared the EPO- and steroid-driven SAGs in terms of their ability to expand Ba/F3 cells. The Ba/F3 cells expressing either of the two EPO-driven SAGs proliferated in the presence of EPO to the same extent as the parental Ba/F3 cells in the presence of IL-3. Of note, the EPO-driven SAG (EPORGCR) expanded Ba/F3 cells by around 10^4-fold more than the steroid-driven counterpart (ΔGCRTmR) after 2 weeks of culture (Figure 2B), indicating that the molecular switch using the EPOR is more efficient than that using the tamoxifen receptor despite the inclusion of the same signal generator (GCR) in the SAGs. Thus, we used EPO-driven SAGs for subsequent experiments.

In vitro effects of the EPO-driven SAGs on human CD34$^+$ cells

To examine whether GCR or c-Mpl is the more suitable signal generator of the EPO-driven SAG, human cord blood CD34$^+$ cells were used as targets. CD34$^+$ cells were transduced with bicistronic retroviral vectors which express the EPO-driven SAG as the first cistron and the EYFP gene as the second cistron. After transduction, 27.3 ± 4.7% of the cells fluoresced (YFP-positive). The transduced CD34$^+$ cells were then cultured in liquid medium in the presence of EPO. The fraction of YFP-positive cells increased over time, and virtually all (>95%) of the cells became YFP-positive during a 2-week culture with EPO. This suggests that the EPO-driven SAGs are able to confer a growth advantage on human CD34$^+$ cells. As shown in Figure 3, although the cells transduced with EPORwt proliferated most quickly, the cell number already began to decrease within 2 weeks after the culture initiation. The cells transduced with EPORGCR grew slowly compared with the others, but began to decrease in number by week 3. On the other hand, the cells transduced with EPORMpl proliferated the longest (1 month) in the presence of EPO and the cell number increased by 10^4-fold over this period.

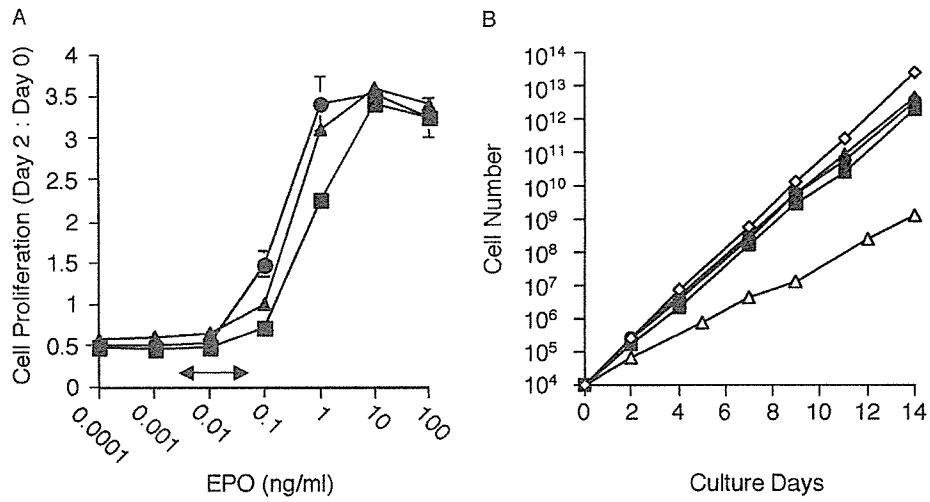

Figure 2. The EPO-driven SAG efficiently stimulates Ba/F3 cell growth. (A) EPO-dependent growth of Ba/F3 cells by introduction of the EPO-driven SAG. BaF3 cells were transduced with the EPORwt (solid triangles), EPORGCR (solid squares) or EPORMpl gene (solid circles) each along with the EYFP gene by bicistronic retroviral vectors. YFP-positive cells were sorted (>98%) and treated with EPO at various concentrations. The proliferation assay (see Materials and Methods) was performed on days 0 and 2, and the ratio of day 2 A_{490}-A_{650} to day 0 A_{490}-A_{650} (means ± SD of triplicate) is shown. The arrow indicates the physiological range of EPO concentrations in human plasma. (B) The EPO-driven SAG triggers higher levels of cell proliferation than the steroid-driven SAG. The parental Ba/F3 cells (open diamonds) were cultured in the presence of IL-3 (10 ng/ml). Ba/F3 cells transduced with the EPORwt (solid triangles), EPORGCR (solid squares), or EPORMpl gene (solid circles) were cultured in the presence of rhEPO (10 ng/ml). Ba/F3 cells transduced with the ΔGCRTmR gene (open triangles) were cultured in the presence of tamoxifen (10^{-7} M). Accumulative data were calculated by means of a triplicate experiment. Experiments were repeated three times and a representative one is shown

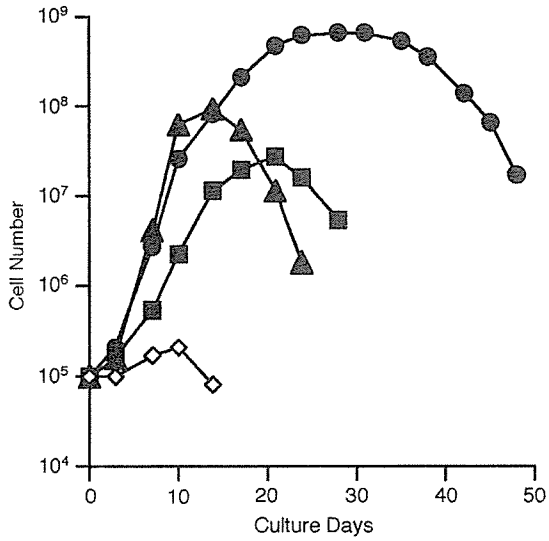

Figure 3. The EPORMpl is the most potent amplifier for human cord blood CD34$^+$ cells. Human cord blood CD34$^+$ cells were transduced with the EPOwt (solid triangles), EPORGCR (solid squares), or EPORMpl gene (solid circles) each along with the EYFP gene by bicistronic retroviral vectors. Untransduced cells are also shown (open diamonds). The cells were then cultured in IMDM supplemented with 10% FBS and 10 ng/ml EPO. Virtually all the cells (>95%) became YFP-positive by week 2. Accumulative data were calculated by means of a triplicate experiment. Experiments were repeated three times and a representative one is shown

Characterization of the c-Mpl signal of SAG

The transduced CD34$^+$ cells were then examined for the expression of c-Kit, a primitive hematopoietic cell marker, by flow cytometry (Figure 4). The c-Kit$^+$ fraction decreased over time, implying that the cells were differentiated during culture. The c-Kit$^+$ fraction in the cells transduced with EPORMpl, however, was relatively high (33%) at week 3 in liquid culture, whereas the c-Kit$^+$ fraction decreased to 10% or lower in the cells transduced with EPORwt or EPORGCR at the same time point. These results demonstrate that the c-Mpl signal preserved more c-Kit$^+$ immature hematopoietic cells than the other signals.

To examine the EPO-driven SAGs for their ability to expand hematopoietic progenitor cells, CD34$^+$ cells transduced with the EPO-driven SAGs were cultured in semisolid (methylcellulose) media in the presence of multiple cytokines (IL-3, IL-6 and SCF) or EPO alone. Table 1 summarizes the results. The cells transduced with the EPO-driven SAGs formed many colonies in the presence of EPO and almost all of them (94–100%) contained the provirus as assessed by individual colony PCR. In contrast, 25–38% of the colonies formed by cells in the presence of multiple cytokines contained the provirus. This result shows that the EPO-driven SAGs are able to confer an EPO-dependent growth advantage at the level of clonogenic progenitor cells. The cells transduced with the EPO-driven SAGs before (day 0) and after (day 7) liquid culture with EPO were placed in semisolid media in the presence of EPO without other cytokines, and the resultant myeloid and erythroid colonies were counted. As shown in Figure 5, during the liquid culture with EPO, the transduction by EPORMpl resulted in the highest levels of clonogenic progenitor cell expansion by more than 10-fold.

We then examined whether cells transduced with the EPO-driven SAGs would show any specific lineage

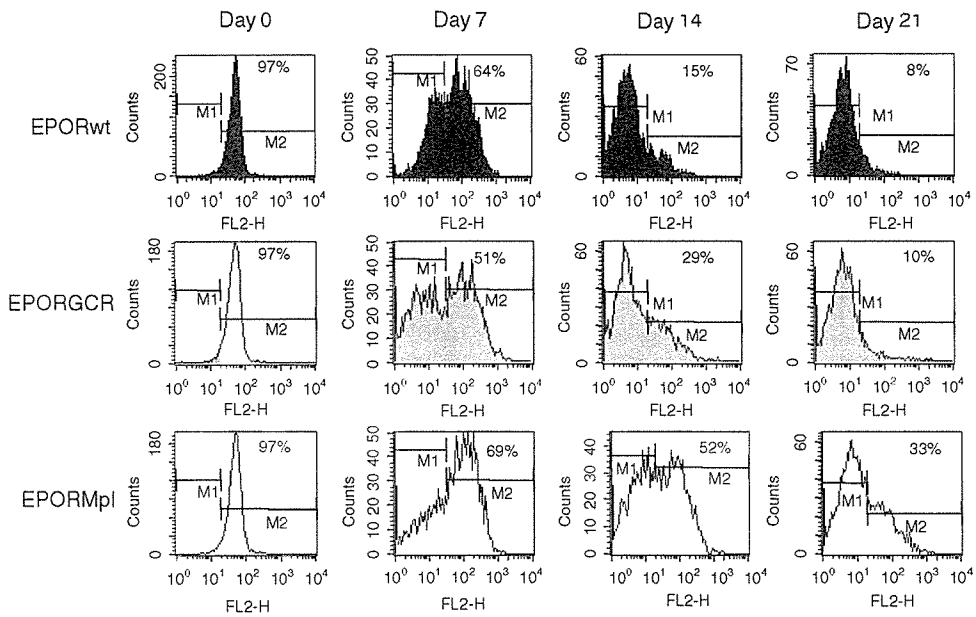

Figure 4. The EPOR-Mpl preserves c-Kit$^+$ cells most efficiently. Human cord blood CD34$^+$ cells were transduced with the EPOwt (black), EPORGCR (gray), or EPORMpl gene (white) by the same retroviral vectors as in Figure 3. The cells were then cultured in IMDM supplemented with 10% FBS and 10 ng/ml EPO. On the indicated days, aliquots of the cells were examined for c-Kit expression by flow cytometry. The percentage of c-Kit$^+$ cells is shown. Experiments were repeated four times and a representative profile is shown

Table 1. Colony formation by human cord blood CD34$^+$ cells transduced with the EPO-driven SAGs

	IL-3 (100 ng/ml) IL-6 (100 ng/ml) SCF (100 ng/ml)		EPO (20 ng/ml)	
Transgene	Number of colonies*	Provirus-positive colonies†	Number of colonies*	Provirus-positive colonies†
EPORwt-YFP	62 ± 11	5/16 (31%)	15 ± 3	15/16 (94%)
EPORGCR-YFP	54 ± 8	6/16 (38%)	24 ± 1	16/16 (100%)
EPORMpl-YFP	54 ± 9	4/16 (25%)	31 ± 6	15/16 (94%)
YFP	49 ± 4	8/16 (50%)	12 ± 1	9/16 (56%)
Untransduced	53 ± 4	ND	17 ± 1	ND

*Colony number out of 200 cells is shown. Each value represents mean ± SD of triplicate culture.
†Individual colony DNA was subjected to PCR for the proviral YFP and genomic β-actin sequences and the ratio of the provirus-positive colony number to the β-actin-positive colony number is shown.

preference after liquid culture with EPO. The transduced CD34$^+$ cells were cultured in liquid medium containing EPO. During the culture, the expression of various differentiation markers was examined by flow cytometry (Figure 6). As expected, the erythroid marker (glycophorin A) was expressed in almost all (93%) cells transduced with EPORwt at day 14. The myeloid marker (CD15) was expressed in 24% of cells transduced with EPORGCR at day 7 (data not shown), but fell to 1% by day 14. Thus, EPORGCR induced very few cells to differentiate toward the myeloid lineage despite the inclusion of the GCR moiety as a signal generator. One reason may be that a point mutation (Y703F) was introduced into the GCR cDNA to attenuate the granulocytic differentiation signal (Figure 1) [3]. On the other hand, cells transduced with EPORMpl expressed all of these markers at relatively high levels at day 14; the megakaryocytic marker (CD41) (46%), glycophorin A (58%) and CD15 (11%). Thus, the cells expanded by the c-Mpl signal showed the most balanced expression of myeloid, erythroid, and megakaryocyte markers. We therefore decided to utilize EPORMpl as an SAG for subsequent *in vivo* experiments in mice.

In vivo expansion of gene-modified cells

Finally, we examined the efficacy of the EPOMpl-type SAG *in vivo* in mice. Murine bone marrow cells were harvested from 5-fluorouracil-treated mice and transduced with the MSCV-based vector expressing both EPORMpl and YFP, or expressing YFP alone as a control. The transduced cells were transplanted into irradiated mice and, after hematopoietic reconstitution, YFP expression was examined in the peripheral blood by flow cytometry to see whether the EPOMpl-transduced cells would increase in response to EPO administration. In mice, however, even drawing a small volume of blood will result in the elevation of endogenous EPO concentrations [23,24]. We also confirmed that sequential blood drawing caused an elevation of endogenous serum EPO concentrations in mice (data not shown). Therefore, drawing blood from the transplanted mice may result in the expansion of transduced hematopoietic cells. To avoid development of anemia due to blood drawing, we

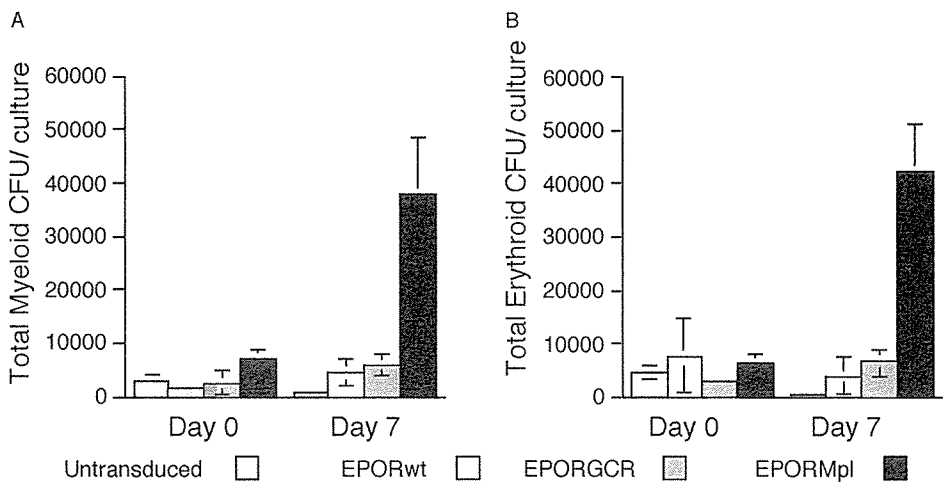

Figure 5. The EPOR-Mpl expands clonogenic progenitor cells most efficiently. Human cord blood CD34$^+$ cells were transduced with the EPOwt, EPORGCR or EPORMpl gene by the same retroviral vectors as in Figure 3. The untransduced and transduced cells were then cultured in IMDM supplemented with 10% FBS and 10 ng/ml EPO for 7 days. The cells before (day 0) and after (day 7) the liquid culture were plated in methylcellulose medium in the presence of EPO alone and the resultant colonies were counted. (A) Total myeloid clonogenic progenitor cell (colony-forming units, CFU) numbers per culture. (B) Total erythroid CFU numbers per culture. Means ± SD of a triplicate experiment are shown. Experiments were repeated three times and a representative one is shown

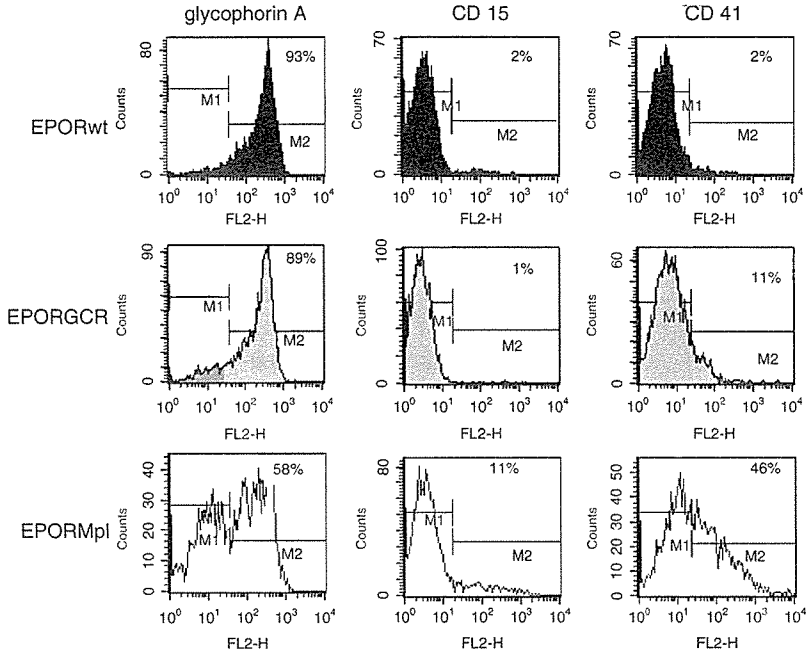

Figure 6. The CD34$^+$ cells expanded by the EPOR-Mpl show the most balanced expression of multilineage surface markers. Human cord blood CD34$^+$ cells were transduced with the EPOwt, EPORGCR, or EPORMpl gene by the same retroviral vectors as in Figure 3. After 14-day liquid culture with 10% FBS and 10 ng/ml EPO, the transduced cells were examined for the expression of glycophorin A (erythroid marker), CD15 (myeloid marker), and CD41 (megakaryocyte marker) by flow cytometry. The percentages of marker-positive cells are shown. Experiments were repeated four times and a representative profile is shown

transfused mice at the time of blood drawing. As a result, the mice did not develop anemia, and thus the elevation of endogenous EPO concentration was prevented.

In the group receiving EPORMpl, YFP-positive cells increased in response to the EPO administration (n = 6), although YFP-positive cells remained unchanged without EPO administration (n = 4) (Figure 7A). A significant increase (paired *t*-test, $p < 0.05$) in YFP-positive cells was observed 4 weeks after the initiation of EPO administration. The increase was attributable to that in granulocytes and monocytes (data not shown). We could not detect any significant change in other lineages. The increase seemed transient, as a significant increase was no longer observed at further time points. On the other hand, in the control group receiving YFP alone without EPORMpl, YFP-positive cells remained unchanged at around 10% in the peripheral blood regardless of EPO administration (n = 6 for a subgroup with EPO, n = 6 for a subgroup without EPO; Figure 7B).

Discussion

Although a few HSC gene therapy trials have proven successful [25,26], most attempts have been hampered by the low efficiency of gene transfer into HSCs. To overcome the problem, we have previously developed a method of selective *in vivo* amplification of transduced hematopoietic cells using a 'selective amplifier gene' (SAG) which encodes a fusion protein consisting of a growth-signal generator and its molecular switch. The prototype SAG encodes a fusion protein between the GCR and the estrogen or tamoxifen receptor, and confers a growth advantage on gene-modified hematopoietic cells in an estrogen- or tamoxifen-inducible fashion *in vivo* [6,7]. In the present study, we developed a new generation SAG which utilizes the EPOR as a molecular switch instead of the steroid receptor. The EPO-driven SAG encodes a fusion protein between the extracellular plus transmembrane domain of the EPOR and the cytoplasmic domain of the GCR or c-Mpl. The results reported here indicated that the SAG utilizing the EPOR as a molecular switch is more efficient for hematopoietic cell proliferation than that utilizing the steroid (or tamoxifen) receptor despite the inclusion of the same signal generator in the SAGs.

Cytokine receptors generate the growth signal through ligand-induced dimerization. Dimerization is necessary but not sufficient for optimal signal generation [27,28]. The EPO-driven SAG might have allowed more effective ligand-induced conformation change than the steroid-driven SAG. Similar to our chimeric receptors, Blau *et al.* developed a cell growth switch that is a cytokine receptor-FK506 binding protein (FKBP) fusion gene to confer inducible proliferation to transduced cells [29,30]. In their system, cytokine receptor signal is turned on by treatment with a synthetic dimerizer FK1012 or its derivatives. However, it remains unclear whether their chimeric protein would allow effective ligand-induced conformation change to the same extent as the EPO-driven SAG.

We also showed that the c-Mpl signal expanded clonogenic progenitor cells (CFU) far more efficiently than the EPOR or GCR signal. In addition, the cells expanded

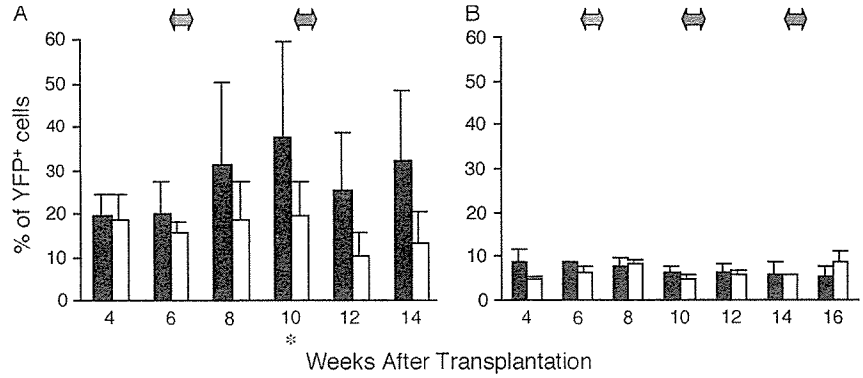

Figure 7. The gene-modified hematopoietic cells can be expanded by treatment with EPO *in vivo* in mice. Murine bone marrow cells were harvested from 5-fluorouracil-treated mice and transduced with the retroviral vector expressing both EPORMpl and YFP, or expressing YFP alone as a control. The transduced cells were transplanted into irradiated mice. The percentages of YFP-positive cells in the peripheral blood are shown for the EPOR-Mpl group (A) or the YFP control group (B). In each group, mice were divided into two subgroups: EPO-treated subgroup (solid bars, 200 IU/kg, three times a week, n = 6 each for A and B) and EPO-untreated subgroup (open bars, n = 4 for A and n = 6 for B). The gray arrows in A and B indicate the week of EPO administration. Means ± SD of each subgroup are shown. The increase in YFP-positive cells in the EPO-treated mice was statistically significant at week 10 (4 weeks after the initiation of EPO administration) ($^*p < 0.05$)

by the c-Mpl signal showed the most balanced expression of myeloid, erythroid, and megakaryocyte markers. Other investigators have also shown that the c-Mpl signal is able to efficiently support the growth of transduced murine bone marrow cells [31]. Taken together, the intracellular signal from c-Mpl may be suitable for reliable expansion of immature hematopoietic cells.

We have demonstrated that EPORMpl can confer an EPO-dependent growth advantage on the transduced hematopoietic cells *in vivo* in a mouse transplantation model. It should be noted that EPORMpl contains the human c-Mpl and may not have worked well in mouse cells. It would be more predictive to examine the efficacy of the EPORMpl in nonhuman primates. We are evaluating the efficacy of EPOMpl-type SAGs in the setting of a nonhuman primate transplantation protocol. In mice, the increase of transduced cells with EPORMpl seemed transient, as was the case with chimeric genes reported by other investigators [32,33]. The method may not result in the selection of transduced cells at the HSC level. The long terminal repeat (LTR) promoter may not express the transgene in HSCs. Alternatively, the c-Mpl signal may not induce proliferation of HSCs. Thus, the selection of transduced cells may occur only within the differentiated progeny of transduced HSCs, not at the level of transduced HSCs themselves. In order to obtain clinically relevant effects, repeated EPO administration would be required. Polycythemia may take place, but it can be treated by occasional phlebotomy safely. Given that our earlier version of SAG utilized estrogen receptor as a molecular switch, we believe that EPO is much safer than estrogen to turn on a molecular switch, since side effects induced by estrogen may not be well treated or controlled.

With the EPO-driven SAG, therapeutic effects may result from continuously elevated levels of endogenous EPO in patients with chronic anemia such as thalassemia. When anemia is ameliorated and endogenous EPO levels return to physiological levels, the positive selection system is then 'automatically' turned off. This 'leave it to patients' system would be convenient. However, a safety concern may be raised regarding leukemogenesis, as the SAG proliferation signal is persistently turned on *in vivo* by endogenous EPO, although physiological levels of EPO will not induce a significant proliferative response. Since a set of EPO-mimetic peptides or a modified EPO such as the erythropoiesis stimulating protein (NESP) has been developed [34,35], it may be possible to develop an EPO-driven SAG containing a mutant EPOR which does not bind to endogenous EPO but binds to the EPO-mimetic peptides or modified EPO.

Acknowledgements

We are grateful to Noriko Nagashima, Aki Takaiwa, and Shintaro Komaba for technical assistance. We acknowledge the supply of RetroNectin from Takara, the supply of rhIL-6, from Ajinomoto and the supply of rhTPO from Kirin. This study was supported by the Ministry of Education, Culture, Sports, Science and Technology of Japan and by the Ministry of Health, Labor and Welfare of Japan.

References

1. Dunbar CE, Cottler-Fox M, O'Shaughnessy JA, *et al.* Retrovirally marked CD34-enriched peripheral blood and bone marrow cells contribute to long-term engraftment after autologous transplantation. *Blood* 1995; **85**: 3048–3057.
2. Ito K, Ueda Y, Kokubun M, *et al.* Development of a novel selective amplifier gene for controllable expansion of transduced hematopoietic cells. *Blood* 1997; **90**: 3884–3892.
3. Matsuda KM, Kume A, Ueda Y, *et al.* Development of a modified selective amplifier gene for hematopoietic stem cell gene therapy. *Gene Ther* 1999; **6**: 1038–1044.
4. Xu R, Kume A, Matsuda KM, *et al.* A selective amplifier gene for tamoxifen-inducible expansion of hematopoietic cells. *J Gene Med* 1999; **1**: 236–244.
5. Nagashima T, Ueda Y, Hanazono Y, *et al.* New selective amplifier genes containing c-Mpl for hematopoietic cell expansion. *Biochem Biophys Res Commun* 2003; **303**: 170–176.

6. Kume A, Koremoto M, Xu R, *et al. In vivo* expansion of transduced murine hematopoietic cells with a selective amplifier gene. *J Gene Med* 2003; **5**: 175–181.
7. Hanazono Y, Nagashima T, Takatoku M, *et al. In vivo* selective expansion of gene-modified hematopoietic cells in a nonhuman primate model. *Gene Ther* 2002; **9**: 1055–1064.
8. Bazan JF. Structural design and molecular evolution of a cytokine receptor superfamily. *Proc Natl Acad Sci U S A* 1990; **87**: 6934–6938.
9. Suzanne LK, Donald NC, William W, *et al.* Proliferation of multipotent hematopoietic cells controlled by a truncated erythropoietin receptor transgene. *Proc Natl Acad Sci U S A* 1996; **93**: 9402–9407.
10. Brandt JR, Avner ED, Hickman RO, *et al.* Safety and efficacy of erythropoietin in children with chronic renal failure. *Pediatr Nephrol* 1999; **13**: 143–147.
11. Itri LM. The use of epoetin alfa in chemotherapy patients: a consistent profile of efficacy and safety. *Semin Oncol* 2002; **29**: 81–87.
12. Borge OJ, Ramsfjell V, Cui L, *et al.* Ability of early acting cytokines to directly promote survival and suppress apoptosis of human primitive $CD34^+$ $CD38^-$ bone marrow cells with multilineage potential at the single-cell level: key role of thrombopoietin. *Blood* 1997; **90**: 2282–2292.
13. Solar GP, Kerr WG, Zeigler FC. *et al.* Role of c-mpl in early hematopoiesis. *Blood* 1998; **92**: 4–10.
14. Kimura S, Roberts AW, Metcalf D, *et al.* Hematopoietic stem cell deficiencies in mice lacking c-Mpl, the receptor for thrombopoietin. *Proc Natl Acad Sci U S A* 1998; **95**: 1195–1200.
15. Kaushansky K. Mpl and the hematopoietic stem cell. *Leukemia* 2002; **16**: 738–739.
16. Gurney AL, Wong SC, Henzel WJ, *et al.* Distinct regions of c-Mpl cytoplasmic domain are coupled to the JAK-STAT signal transduction pathway and Shc phosphorylation. *Proc Natl. Acad Sci U S A* 1995; **92**: 5292–5296.
17. Pear WS, Nolan GP, Scott ML, *et al.* Production of high-titer helper-free retroviruses by transient transfection. *Proc Natl Acad Sci. U S A* 1993; **90**: 8392–8396.
18. Kralovics R, Sokol L, Prchal JT. Absence of polycythemia in a child with a unique erythropoietin receptor mutation in a family with autosomal dominant primary polycythemia. *J Clin Invest* 1998; **102**: 124–129.
19. Hawley RG, Lieu FH, Fong AZ, *et al.* Versatile retroviral vectors for potential use in gene therapy. *Gene Ther* 1994; **1**: 136–138.
20. Takatoku M, Kametaka M, Shimizu R, *et al.* Identification of functional domains of the human thrombopoietin receptor required for growth and differentiation of megakaryocytic cells. *J Biol Chem* 1997; **272**: 7259–7263.
21. Huang Z, Tamura M, Sakurai T, *et al. In vivo* transfection of testicular germ cells and transgenesis by using the mitochondrially localized jellyfish fluorescent protein gene. *FEBS Lett* 2000; **487**: 248–251.
22. Hanenberg H, Xiao XL, Dilloo D, *et al.* Colocalization of retrovirus and target cells on specific fibronectin fragments increases genetic transduction of mammalian cells. *Nat Med* 1996; **2**: 876–882.
23. Oishi A, Sakamoto H, Shimizu R, *et al.* Evaluation of phlebotomy-induced erythropoietin production in the dog. *J Vet Med Sci* 1993; **55**: 51–58.
24. Chapel SH, Veng-Pedersen P, Schmidt RL, *et al.* Receptor-based model accounts for phlebotomy-induced changes in erythropoietin pharmacokinetics. *Exp Hematol* 2001; **29**: 425–431.
25. Cavazzana-Calvo M, Hacein-Bey S, de Saint Basile G, *et al.* Gene therapy of human severe combined immunodeficiency (SCID)-X1 disease. *Science* 2000; **288**: 669–672.
26. Aiuti A, Slavin S, Aker M, *et al.* Correction of ADA-SCID by stem cell gene therapy combined with nonmyeloablative conditioning. *Science* 2002; **296**: 2410–2413.
27. Livnah O, Stura EA, Middleton SA, *et al.* Crystallographic evidence for preformed dimers of erythropoietin receptor before ligand activation. *Science* 1999; **283**: 987–990.
28. Remy I, Wilson IA, Michnick SW. Erythropoietin receptor activation by a ligand-induced conformation change. *Science* 1999; **283**: 990–993.
29. Blau CA, Peterson KR, Drachman JG, *et al.* A proliferation switch for genetically modified cells. *Proc Natl Acad Sci U S A* 1997; **94**: 3076–3081.
30. Richard RE, Wood B, Zeng H, *et al.* Expansion of genetically modified primary human hemopoietic cells using chemical inducers of dimerization. *Blood* 2000; **95**: 430–436.
31. Zeng H, Masuko M, Jin L, *et al.* Receptor specificity in the self-renewal and differentiation of primary multipotential hemopoietic cells. *Blood* 2001; **98**: 328–334.
32. Jin L, Zeng H, Chien S, *et al. In vivo* selection using a cell-growth switch. *Nat Genet* 2000; **26**: 64–66.
33. Neff T, Horn PA, Valli VE, *et al.* Pharmacologically regulated *in vivo* selection in a large animal. *Blood* 2002; **100**: 2026–2031.
34. Wrighton NC, Farrell FX, Chang R, *et al.* Small peptides as potent mimetics of the protein hormone erythropoietin. *Science* 1996; **273**: 458–464.
35. Macdougall IC. Novel erythropoiesis stimulating protein. *Semin Nephrol* 2000; **20**: 375–381.

Cancer Chemother Pharmacol (2004) 53: 129–132
DOI 10.1007/s00280-003-0707-8

ORIGINAL ARTICLE

Kiyoshi Mori · Yukari Kamiyama · Tetsuro Kondo
Yasuhiko Kano · Keigo Tominaga

Phase II study of the combination of vinorelbine and cisplatin in advanced non-small-cell lung cancer

Received: 14 April 2003 / Accepted: 31 July 2003 / Published online: 7 November 2003

Abstract *Purpose*: To evaluate the efficacy and safety of combination chemotherapy with cisplatin and vinorelbine for the treatment of previously untreated patients with advanced non-small-cell lung cancer (NSCLC). *Patients and methods*: Eligible patients were those with measurable NSCLC. They were treated with two or more cycles of a regimen consisting of vinorelbine 25 mg/m^2 on days 1 and 8 and cisplatin 80 mg/m^2 on day 1 every 3 weeks. *Results*: A total of 45 patients were enrolled. The response rate was 51.1% (23/45; 95% CI 35.8% to 66.3%). The median survival was 286 days with a 1-year survival rate of 40%. The median number of treatment cycles was 2. The major toxic effect was neutropenia of grade 3 or higher (84%). Nonhematological toxicities, including vomiting (62%), were mild (grade 2 or less). There were no treatment-related deaths. *Conclusion*: The high response rate and good tolerability proved this combination therapy to be a safe and effective treatment for advanced NSCLC.

Keywords Non-small-cell lung cancer · Vinorelbine · Cisplatin · Phase II study

Introduction

Vinorelbine ditartrate [1], a vinca alkaloid derivative, shows antitumor activity mainly by inhibiting microtubule polymerization in tumor cells just as other vinca alkaloid drugs do [2, 9]. Clinical studies of vinorelbine (VNR) have shown a good therapeutic outcome in non-small-cell lung cancer (NSCLC) and breast cancer, and a reduction in peripheral neuropathy that occurs frequently with vinca alkaloids [5, 7, 10, 12]. The combination of VNR and cisplatin (CDDP) (VP therapy) has shown a synergistic effect in vitro, while the main side effects are different between the drugs [4]. A phase I-II study has demonstrated efficacy of this combination in NSCLC [3]. VP therapy is considered a promising combination regimen for NSCLC on account of its higher response rate and longer survival compared with VNR or CDDP alone, or CDDP combined with vindesine [8, 17].

In clinical studies performed in Europe and the US, patient compliance rate was as low as 50% or less with regard to VNR when VP therapy, as VNR 25 mg/m^2 weekly and CDDP 80 mg/m^2 on day 1, was repeated every 4 weeks. This indicates the need to reconsider the dosing schedule of VNR [17]. Another dosing schedule for VP therapy (VNR 20 to 30 mg/m^2 on days 1 and 8 and CDDP 80 mg/m^2 on day 1 every 3 weeks) showed almost complete compliance and was found to be beneficial since the response rate was 28.3% to 56.7% and the survival 9.2 to 10.6 months [6, 13, 15, 17].

VP therapy is an effective regimen against advanced NSCLC. A multicenter joint phase III study is being planned in Japan to compare four regimens for advanced NSCLC: CDDP plus irinotecan used as a reference arm, CDDP plus VNR every 3 weeks, CDDP plus gemcitabine and carboplatin plus paclitaxel. A phase II study of VP therapy has not been conducted in Japan. We therefore carried out a phase II study of VNR 25 mg/m^2 on days 1 and 8 plus CDDP 80 mg/m^2 on day 1 given every 3 weeks in advanced NSCLC to evaluate the efficacy and safety of VP therapy.

Patients and methods

Patient selection

Patients eligible for the study were those admitted to our hospital between August 1999 and October 2001 who were histologically or

This work was supported in part by a grant-in-aid from the Ministry of Health and Welfare (Tokyo, Japan) and from the Second Term Comprehensive 10-Year Strategy for Cancer Control.

K. Mori (✉) · Y. Kamiyama · T. Kondo · Y. Kano
K. Tominaga
Department of Thoracic Diseases, Tochigi Cancer Center,
4-9-13 Yonan, Utsunomiya, 320-0834 Tochigi,
Japan
E-mail: kmori@tcc.pref.tochigi.jp
Tel.: +81-28-6585151
Fax: +81-28-6585669

cytologically diagnosed as having NSCLC and who were in clinical stage III or IV with unresectable disease, or in whom radiotherapy with curative intent was not possible, including those who had pleural effusion and dissemination, those with intrapulmonary metastasis within the ipsilateral lobe, those in whom the irradiation field exceeded one-half of one lung, those with metastasis to the contralateral hilar lymph nodes, and those with reduced lung function. None of the patients had received prior therapy. Other eligibility criteria included expected survival of 12 weeks, age ≤ 75 years, Eastern Cooperative Oncology Group performance score (PS) of 0–2, measurable lesions, adequate hematological function (WBC ≥4000/mm^3, platelet count ≥100,000/mm^3, hemoglobin ≥10 g/dl), renal function (serum creatinine ≤ 1.5 mg/dl, creatinine clearance ≥60 ml/min), and hepatic function (total serum bilirubin ≤ 1.5 mg/dl, serum GOT and serum GPT less than twice the upper limit of normal). Written informed consent was obtained from every patient with the statement that the patient was aware of the investigational nature of this treatment regimen. Pretreatment evaluation included medical history, physical examination, complete blood count, serum biochemical analyses, chest roentgenogram, electrocardiogram and urinalysis. All patients underwent radionuclide bone scan and computerized tomography of the brain, thorax, and abdomen.

Treatment

The anticancer drugs were administered via the intravenous route, VNR 25 mg/m^2 (Navelbine, Kyowa Hakko Kogyo) on days 1 and 8 and CDDP 80 mg/m^2 (Randa, Nippon Kayaku) on day 1. This combination therapy repeated every 3 weeks constituted a cycle of treatment. The minimal number of cycles to be evaluated was two. On day 8, the physician examined the patient and evaluated the development of adverse events, and if leukocytes had decreased to below 2000/mm^3, platelets had decreased to below 75,000/mm^3 or fever with infection had occurred, administration of VNR on that day was withheld at the discretion of the physician. To proceed with the second and subsequent cycles, patients were required to have a neutrophil count ≥1500/mm^3 and a platelet count ≥100,000/mm^3. Those patients receiving granulocyte colony-stimulating factor (G-CSF) were observed for 3 days after the final dose of G-CSF to ensure that their neutrophil count was 1500/mm^3 or more. Serum creatinine levels were required to be below the upper limit of normal and serum GOT/GPT levels below twice the upper limit of normal. In the presence of liver dysfunction due to apparent liver metastasis, however, serum GOT and GPT levels were required to be below three times the upper limit of normal. If fever occurred or if the PS advanced to grade 3 or worse, the subsequent cycle was postponed until the temperature fell below 38°C or until the PS returned to 2 or less. In the presence of grade 2 peripheral neuropathy dosing was temporarily postponed; with improvement to grade 1 or less treatment was cautiously resumed, but medication was discontinued if 6 weeks passed without any improvement. Peripheral neuropathy (including transient) grade 3 or higher required discontinuation of treatment. For the third and subsequent cycles, VNR or CDDP was decreased by 25% in accordance with the treatment-related adverse events observed during the preceding cycle. Steroid and HT_3-antagonist were administered to prevent nausea and vomiting.

Target population size and interim analysis

Simon's two-stage minimax design [16] was used to estimate the number of patients required for interim and final analyses at a threshold response rate (P_0) of 0.20, an expected response rate (P_1) of 0.40, $\alpha = 0.05$ and $\beta = 0.10$. If the interim analysis revealed 6 responding patients out of 24, recruitment would be continued until the target population size was achieved. The combination therapy was considered effective if 14 or more of 45 patients showed response in the final analysis.

Since an interim response rate of 48.1% (13/27) [11] was obtained, it was necessary to enroll up to 45 patients for the final analysis.

Evaluation of response and toxicity

Response and toxicity were evaluated on the basis of tumor images obtained by CT and other techniques, laboratory data and subjective/objective symptoms before, during and after administration of the study drugs and during the period from completion of treatment to the final analysis. Measurable disease parameters were determined every 4 weeks by various means such as computerized tomography. Evaluation was made in compliance with Response Evaluation Criteria in Solid Tumors (RECIST) guidelines [14] for antitumor activity and with NCI Common Toxicity Criteria version 2 for safety. The Institutional Ethical Review Committee gave approval to the study.

Results

Patient characteristics

Table 1 gives characteristics of the patients included. Their median age was 59.5 years (range 35 to 75 years). Male, PS 1 and adenocarcinoma predominated. There were 26 patients (58%) with stage IV disease and 19 (42%) with stage IIIB disease.

Treatments administered

The total number of cycles administered was 126 with a median of two per patient (ranging from one to four cycles; Table 2) and 43 patients received two cycles or more. In the two patients who received fewer than two cycles, treatment was discontinued because of CDDP-induced renal dysfunction in one and patient refusal in the other. Patients who completed two cycles or more accounted for 96% of patients (43/45). Except the two patients who received only one cycle, the every-3-week

Table 1 Patient characteristics

Eligible patients (*n*)	45
Age (years)	
Median	59.5
Range	35–75
Sex (*n*)	
Male	34
Female	11
Performance status (*n*)	
0	11
1	32
2	2
Histology (*n*)	
Adenocarcinoma	30
Squamous cell carcinoma	9
Other	6
Stage (*n*)	
IIIB	19
IV	26

Table 2 Efficacy of treatment ($n=45$)

No. of cycles	
Median	2.0
Range	1–4
Response	
Partial response	23
No change	21
Not evaluable	1
Response Rate (%)	51.1
95% CI (%)	35.8–66.3
1-year survival rate (%)	40

dosing schedule was adhered to by 88% of patients (38/43) in the second cycle, 68% (17/25) in the third and 92% (12/13) in the fourth, with a total of 83% (67/81). Only in two cycles was VNR withheld on day 8. The dose of VNR was reduced in 9% of dose administrations (22/250) and the does of CDDP was reduced in 8% (10/126). The planned dose intensities were 16.7 mg/m^2 per week for VNR and 26.7 mg/m^2 per week for CDDP while the actual dose intensities were 16.4 and 24.7 mg/m^2 per week, respectively. The median delivered dose intensity for CDDP (day 1) and VNR (days 1 and 8) of each course together was 90% or more (Table 3).

Efficacy of treatment

Of the 45 patients, 23 showed a partial response, 21 showed no change and 1 was not evaluable (Table 2). The response rate was 51.1% (23/45; 95% CI 35.8% to 66.3%; Table 2). The nonevaluable patient died of sudden hemoptysis on the 22nd day after the start of the second cycle (43rd day after the start of treatment) and could not be evaluated. Ten patients were alive at the time of this report. The time to progressive disease was 172 days and the median survival was 286 days (95% CI 248 to 404 days; Table 2). The 1-year survival rate was 40%.

Table 3 Median delivered dose intensity

	Median dose intensity (%)			
	Course 1	Course 2	Course 3	Course 4
CDDP	100	98.8	96	92.3
VNR				
Day 1	100	98.6	95.5	93.8
Day 8	97.8	98.6	95.5	93.8

Toxicities

Table 4 lists toxicities observed during the study. Hematological and blood biochemical reactions included a high incidence of leukopenia and neutropenia, i.e. leukopenia and neutropenia of grade 3 or higher occurred in 73% of patients (33/45) and 84% (38/45), respectively. Neutropenia-associated fever was limited to two patients. All neutropenic patients recovered upon treatment with G-CSF. Platelets decreased in 4% of patients (2/45). Creatinine was temporarily elevated in 15.6% (7/45).

Subjective and objective symptoms observed were of grade 2 or less and included vomiting in 77.8% of patients (35/45), hiccough in 33.3% (15/45), constipation in 40% (18/45), diarrhea in 22% (10/45), rash in 31.1% (14/45) and injection site reaction in 26.7% (12/45). All of these toxicities disappeared or improved with symptomatic treatment. There were no toxic deaths.

Discussion

As for the VP regimen for advanced NSCLC, the every-3-week dosing schedule has been tried in several medical facilities [6, 13, 15, 17]. Table 5 summarizes the clinical outcomes of every-3-week VP therapy reported in the literature and in this study. Response rates range from 28% to 57% and median survival is approximately 10 months. The results are similar among the studies.

In 96% of patients (43/45), two or more cycles of VP therapy were administered. The every-3-week dosing

Table 4 Toxicities ($n=45$)

Toxicity	Grade (Common Toxicity Criteria)				Grade 3/4 (%)
	1	2	3	4	
Leukopenia	4	3	25	8	33 (73%)
Neutropenia	2	2	13	25	38 (84%)
Anemia	12	3	1	4	5 (11%)
Thrombocytopenia	5	1	2	0	2 (4%)
Creatinine	5	2	0	0	–
Vomiting	29	6	0	0	–
Hiccough	15	0	0	0	–
Constipation	13	5	0	0	–
Diarrhea	9	1	0	0	–
Rash	10	4	0	0	–
Neuropathy	4	0	0	0	–
Injection site reaction	4	8	0	0	–
Alopecia	3	0	0	0	–

Table 5 Outcomes of studies of VP therapy (VNR days 1 and 8, CDDP day 1, every 3 weeks)

Reference	VNR (mg/m^2)	CDDP (mg/m^2)	Response	Median survival time (months)
4	25	80	28.3% (28/99)	9.2
10	25	80	56.7% (42/74)	10
11	20–25	80	46.7% (14/30)	10.6
1	30	80	36.2% (47/130)	–
Present study	25	80	51.1% (23/45)	9.6

schedule was adhered to in 85% of all cycles administered. In cycles in which noncompliance was seen, medication was postponed to the 4th to 5th week because, in most cases, the neutrophil count in the 3rd week failed to meet the criterion for going on to subsequent cycles. The planned dose intensity was almost attained since the actual dose intensity was 16.4 mg/m^2 per week for VNR and 24.7 mg/m^2 per week for CDDP, accounting for 98% and 93% of the planned values, respectively [13].

Most adverse reactions were hematological. In particular, leukopenia and neutropenia of grade 3 or worse occurred in 73% and 84% of 45 patients, respectively. Others have reported the incidence of leukopenia of grade 3 or worse to be 8% to 33% [6, 13, 17]. Although the difference in patient characteristics hinders simple comparison and analysis of these data, it can be said that leukopenia was more frequent in our study. The leukocyte count improved rapidly upon treatment with G-CSF. Nonhematological toxicities were mild and adverse reactions of grade 3 or higher were not noted.

The combination of VNR 25 mg/m^2 on days 1 and 8 and CDDP 80 mg/m^2 on day 1 was administered every 3 weeks to 45 patients with advanced NSCLC in this phase II study. The response rate was 51.1%; the main adverse effect was neutropenia. The high response rate and good tolerability indicate that this combination therapy is a safe and effective treatment for advanced NSCLC. Its usefulness will be further verified in phase III studies.

References

1. Adam Z, Coupkova H, Kolek V, et al (1995) Vinorelbine and cisplatin in the treatment of advanced non-small-cell lung cancer: results of a multicenter Czech study. Acta Med Austriaca 22:120–124
2. Berthaud P, Le Chevalier LT, Ruffie P, et al (1992) Phase I-II study of vinorelbine (Navelbine) plus cisplatin in advanced non-small cell lung cancer. Eur J Cancer 28A:1863–1865
3. Binet S, Fellous A, Lataste H, Krikorian A, Couzinier JP, Meininger V (1989) In situ analysis of the action of navelbine on various types of microtubules using immunofluorescence. Semin Oncol 16 [Suppl 4]:5–8
4. Bretti S, Berruti A, Gorzegno G, et al (1996) Multicenter phase II trial of intermediate dose cisplatin and vinorelbine in inoperable non-small cell lung cancer patients. Lung Cancer 14:353–360
5. Canobbio L, Boccardo F, Pastorino G, et al (1989) Phase II study of Navelbine in advanced breast cancer. Semin Oncol 16 [Suppl 4]:33–36
6. Chevalier TL, Brisgand D, Douillard JY, et al (1994) Randomized study of vinorelbine and cisplatin versus vindesine and cisplatin versus vinorelbine alone in advanced non-small cell lung cancer: results of a European multicenter trial including 612 patients. J Clin Oncol 12:360–367
7. Depierre A, Lemarie E, Dabouis G, Garnier G, Jacoulet P, Dalphin JC (1989) Efficacy of Navelbine (NVB) in non-small cell lung cancer (NSCLC). Semin Oncol 16 [Suppl 4]:26–29
8. Depierre A, Lemarie E, Dabouis G, Garnier G, Jacoulet P, Dalphin JC (1991) A phase II study of Navelbine (vinorelbine) in the treatment of non-small cell lung cancer (NSCLC). Am J Clin Oncol 14:115–119
9. Fellous A, Ohayon R, Vacassin T, et al (1989) Biochemical effects of Navelbine on tubulin and associated proteins. Semin Oncol 16 [Suppl 4]:9–14
10. Frontini L, Candido P, Cattaneo MT, et al (1996) Cisplatin-vinorelbine combination chemotherapy in locally advanced non-small cell lung cancer. Tumori 82:57–60
11. Gebbia V, Caruso M, Valenza R, et al (1994) Vinorelbine plus cisplatinum for the treatment of stage IIIB and IV non-small cell lung carcinoma. Anticancer Res 14:1247–1250
12. Gomi K, Ohno H, Nomura K, Okabe M, Kobayashi K, Niitani H (1986) Kinetic analysis of combination effect of Navelbine (KW-2307) with cisplatin against human lung adenocarcinoma PC-12 cell in culture. Jpn J Cancer Res 83:532–539
13. Kusunoki Y, Furuse K, Yamori S, et al (1995) Randomized phase II study of vinorelbine (VRB) vs vindesine (VDS) in previously untreated non-small cell lung cancer (NSCLC) (abstract 1071). Proc Am Soc Clin Oncol 14:353
14. Mori K, Kamiyama Y, Kondoh T, Tominaga K (2002) Phase II study of combined vinorelbine plus cisplatin for advanced non-small cell lung cancer (an interim report). Jpn Cancer Chemother 29:405–410
15. Potier P (1989) The synthesis of navelbine prototype of a new series of vinblastine derivatives. Semin Oncol 16 [Suppl 4]:2–4
16. Simon R (1989) Optimal two-stage designs for phase II clinical trial. Control Clin Trial 10:1–10
17. Wozniak AJ, Crowley JJ, Balcerzak SP, et al (1998) Randomized trial comparing cisplatin with cisplatin plus vinorelbine in the treatment of advanced non-small-cell lung cancer: a Southwest Oncology Group study. J Clin Oncol 16:2459–2465